

Supporting Information for

Small molecule perimeter defense in entomopathogenic bacteria

Jason M. Crawford^{a,1}, Cyril Portmann^{a,1}, Xu Zhang^b, Maarten B.J. Roeflaers^b, and Jon Clardy^{a,b,2}

a. Department of Biological Chemistry & Molecular Pharmacology, Harvard Medical School, 240 Longwood Avenue, Boston, MA 02115.

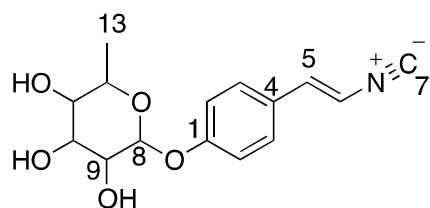
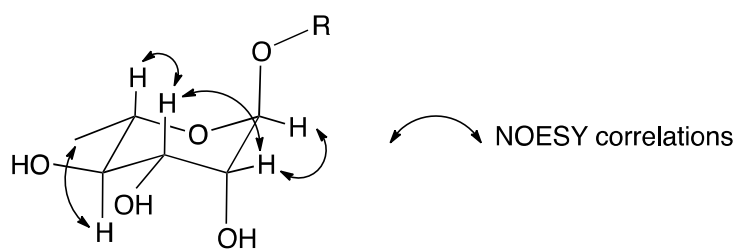
b. Department of Chemistry & Chemical Biology, Harvard University, 12 Oxford Street, Cambridge, MA 02138.

1. J.M.C. and C.P. contributed equally to this work.

2. To whom correspondence may be addressed. Email: jon_clardy@hms.harvard.edu

Table S1. ^1H and ^{13}C NMR Data (400 MHz, $\text{DMSO-}d_6$) for byelyankacin (**2**).

C/H no.	δ_{C}	δ_{H} (J in Hz)	COSY	HMBC	NOESY
1	156.8, qC				
2	116.4, CH	7.04, d (8.8)	3	1, 2, 4	8
3	128.2, CH	7.48, d (8.8)		1, 3, 5	5, 6
4	126.1, qC				
5	135.7, CH	7.11, d (14.4)	6	3, 6	
6	109.6, CH	6.78, d (14.4)		4, 5, 7	
7	163.7, qC				
8	97.8, CH	5.42, d (1.7)	9	1, 9	9
9	69.7, CH	3.83, m	10	10, 11	
10	70.0, CH	3.63, dd (9.3, 3.3)	11	8, 11	11, 12
11	71.4, CH	3.28, dd (9.3, 9.3)	12	12, 13	13
12	69.2, CH	3.42, m	13	10, 11	
13	17.5, CH_3	1.09, d (6.2)		11, 12	

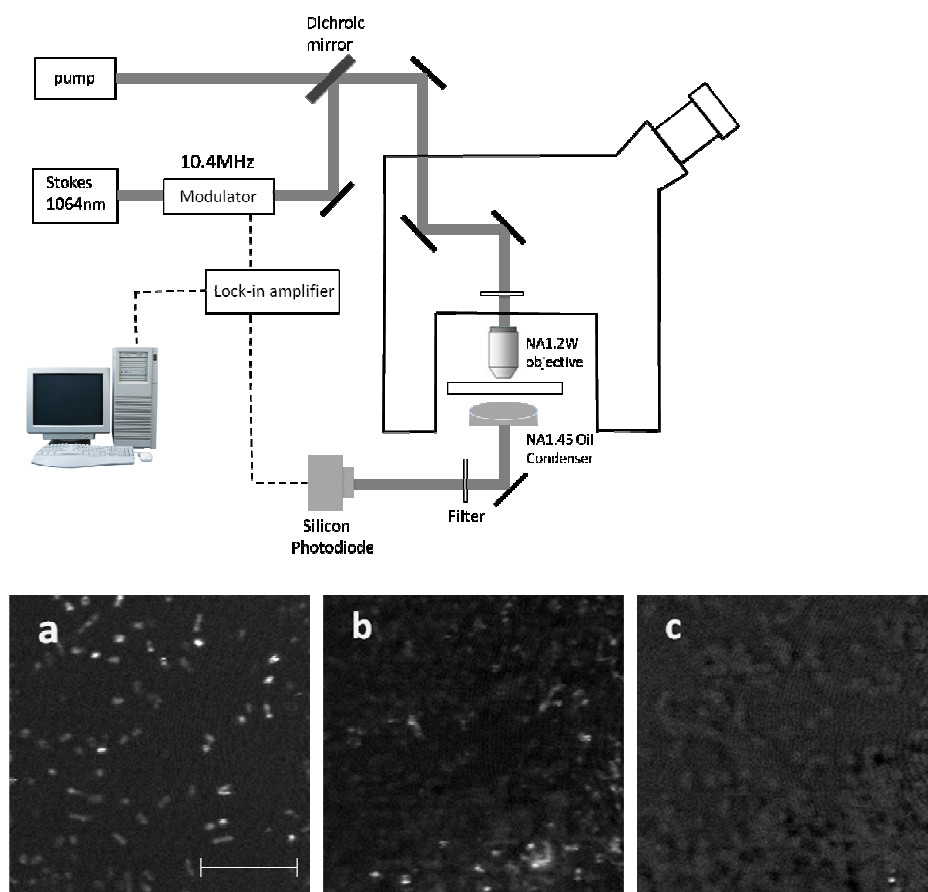
**byelyankacin**

Relative configuration and NOESY correlations for the rhamnopyranoside moiety of byelyankacin.

Byelyankacin (2) MS. HR-MS: (ESI) calcd for $\text{C}_{15}\text{H}_{17}\text{NO}_5\text{Na}$ 314.1004 $[\text{M}+\text{Na}]^+$, found 314.1012.

$[\alpha]_{\text{D}}^{24.5}$ -135 (c 0.1, MeOH).

Figure S1. Top: Stimulated Raman scattering (SRS) microscopy. In SRS microscopy, two laser beams are used to excite the target molecules. The difference frequency between the two laser beams can be tuned to match the vibrational frequency of the molecules. The experimental schematic is shown below. A 1064 nm Nd:YO₄ laser delivering 6ps laser pulse train at the repetition rate of 76 MHz is used as one excitation beam (Stokes beam) and modulated at 10.4 MHz. The other excitation beam (pump beam) is provided by the signal output of the OPO (optical parametric oscillator) synchronously pumped by the frequency doubled Nd:YO₄ laser at the wavelength of 532 nm. The wavelength of the pump beam is tunable to target molecules with different vibrational information. The two excitation beams are overlapped in space and time, sent into the Olympus microscope and focused by a water immersion objective (1.2NA 60×W) onto the sample. The transmitted beams are collected through a high NA condenser onto the 1 cm² silicon photodiode with bias voltage at 64 V after filtering out the Stokes beam. The signal is extracted by a lock-in amplifier (SR844RF, Stanford Research Systems) at 10.4 MHz and fed into the computer system. **Bottom: SRS microscopy analyzing the spatial distribution of the isonitrile functional group in *E. coli* cells heterologously producing rhabduscin [a] and aglycone 3 [b] versus a control vector [c].** Aliquots of stationary phase *E. coli* cells were visualized directly without further manipulation on poly-L-lysine coated microscope slides. As shown previously in Figure 3 as a separate experiment, rhabduscin localizes to the periphery of the bacterial cells. Aglycone 3 appears to exhibit qualitatively less peripheral localization, suggesting that rhabduscin's sugar substituent contributes to rhabduscin placement. The control cells showed very little background signal.

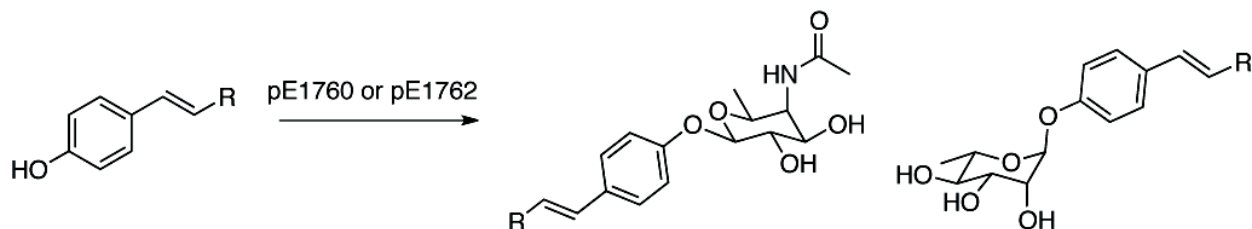


[a] pEPI.IsnAB-GT1762
[b] pEPI.IsnAB
[c] pET-Duet1 control

scale bar = 10 μ m

Table S2. Probing the specificity of GT1760 (Plu1760) and GT1762 (Plu1762) by precursor directed biosynthesis.

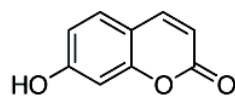
Precursor	pEGT1760		pEGT1762	
	Product	Conversion	Product	Conversion
1a	2a	< 1%	2a	3%
	3a	not detected	3a	not detected
1b	2b	71%	2b	46%
	3b	13%	3b	42%
1c	2c	not detected	2c	not detected
	3c	not detected	3c	not detected
1d	2d	not detected	2d	not detected
	3d	not detected	3d	not detected
1e	2e	not detected	2e	not detected
	3e	not detected	3e	not detected
1f	2f	61%	2f	93%
	3f	not detected	3f	not detected
1g	2g	< 1%	2g	1%
	3g	not detected	3g	< 1%



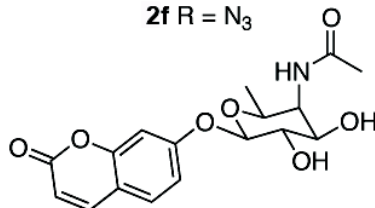
1a R = Ac
1b R = CN
1c R = CH(CN)₂
1d R = NO₂
1e R = COOH
1f R = N₃

2a R = Ac
2b R = CN
2c R = CH(CN)₂
2d R = NO₂
2e R = COOH
2f R = N₃

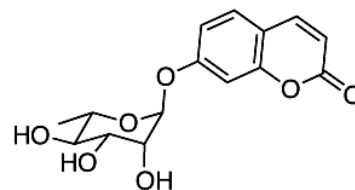
3a R = Ac
3b R = CN
3c R = CH(CN)₂
3d R = NO₂
3e R = COOH
3f R = N₃



1g



2g



3g

Figure S2. Top: Mosher ester reaction scheme with rhabduscin. Bottom: C₁₈ RP-LC/MS analysis of Mosher ester reaction. Crude Mosher ester reaction of rhabduscin with (*S*)-MTPA-Cl (A) and (*R*)-MTPA-Cl (B). The ultraviolet absorption (280 nm) trace is shown. Poor solubility of rhabduscin in coupling solvents led to a poor yield, but enough product was obtained for advanced Mosher ester analysis. Purified rhabduscin-formamide *R*-Mosher ester product (M4, C) from (A), and purified rhabduscin-formamide *S*-Mosher ester product (M4, D) from (B). Baseline separation of M3 and M5 in (A) enabled a rough product ratio to be estimated (M3:M5 was obtained in an approximately 8:2 ratio). M2, 7.1 min, [M+H]⁺ = 351, [M-H]⁻ = 349; M1, 10.3 min, [M+H]⁺ = 333, [M-H]⁻ = 331; M4, 14.4 min, [M+H]⁺ = 567, [M-H]⁻ = 565; M6, 14.6 min, [M+H]⁺ = 567, [M-H]⁻ = 565; M3, 17.3 min, [M+H]⁺ = 549, [M-H]⁻ = 547; M5, 17.4 min, [M+H]⁺ = 549, [M-H]⁻ = 547.

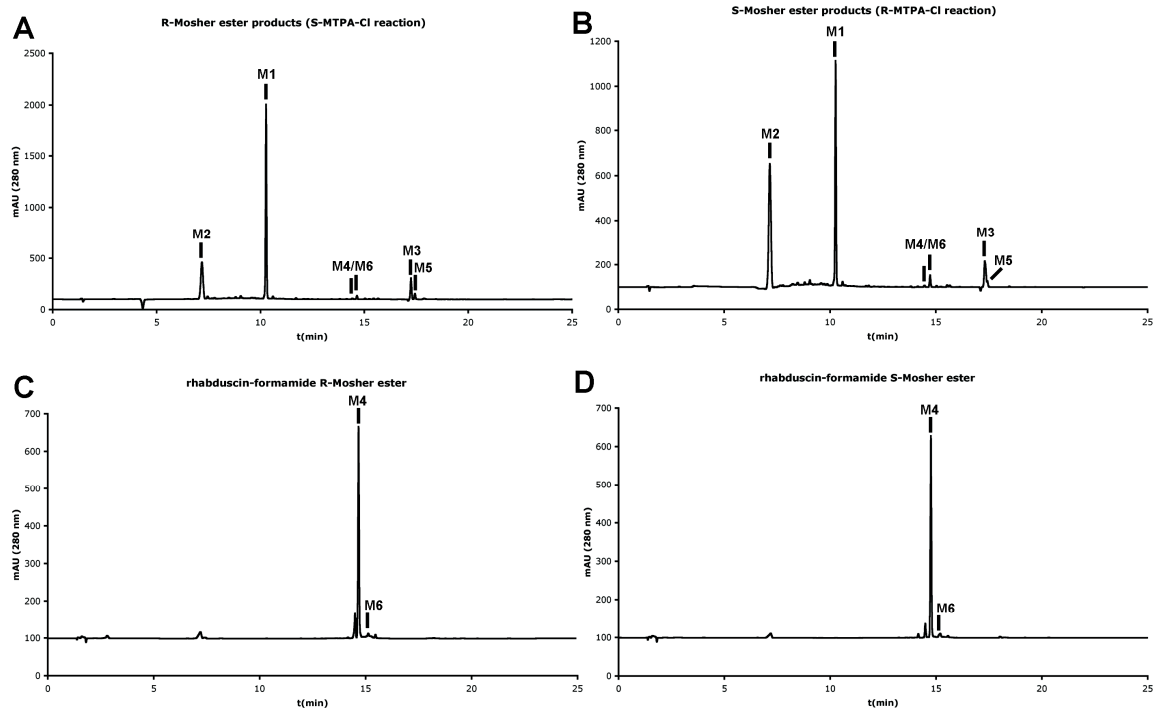
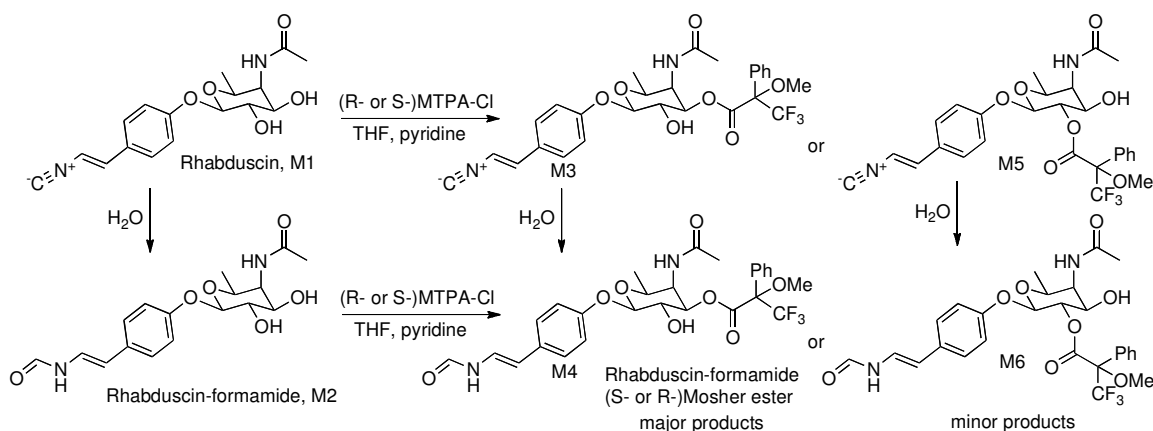


Table S3. The rhabduscin-formamide (*R*- and *S*-) Mosher esters (*R*-M4 and *S*-M4) were analyzed by one-dimensional (^1H) and two-dimensional (gCOSY) NMR in CD_3OD . The rhabduscin-derived proton signals are shown. w, weak signal.

		Rhabduscin-formamide R-Mosher ester		Rhabduscin-formamide S-Mosher ester	
Unit	Position	^1H	gCOSY	^1H	gCOSY
Tyrosyl-derived unit	1				
	2/2'	7.02 d (8.6)	3	7.03 d (8.6)	3
	3/3'	7.30 m	2	7.30 m	2
	4				
	5	7.41 m	6	7.40 m	6
	6	6.26 d (14.7)	5	6.26 d (14.7)	5
Sugar	8	4.98 d (7.6)	9	4.99 d (7.6)	9
	9	3.95 dd (7.8, 10.6)	8, 10	4.05 m	8, 10
	10	5.36 dd (4.9, 10.6)	9, 11	5.23 dd (5.1, 10.3)	9, 11
	11	4.62 dd (4.6, 0.9)	10	4.64 dd (5.0, 1.2)	10, 12 w
	12	4.07 dq (1.2, 6.2)	13	4.05 m	11 w, 13
	13	1.19 d (6.3)	12	1.17 d (6.3)	12
N-acetyl	14				
	15	1.99 s		1.84 s	

Figure S3. Advanced Mosher ester analysis of rhabduscin. (Left) The carbon numbering is mapped onto the *S*- or *R*-rhabduscin-formamide Mosher ester. (Right) δ_{S-R} advanced Mosher ester values, supporting that C10 in the amidoglycosyl ring adopts the *R*-configuration. The small positive value marked in red at C11 was an exception to the rule, as one of the proton resonance differences can occasionally be an exception to the trend.

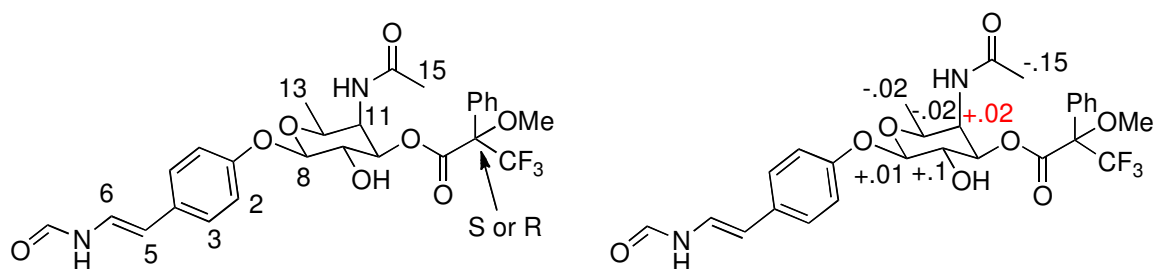


Figure S4. Top: Inhibition curve of mushroom tyrosinase for rhabduscin (**1**), byelyankacin (**2**), aglycones **3** (aglycone-NC), **6** (aglycone-CN), and **12** (aglycone-N3), and kojic acid. **Bottom:** Inhibition of hemolymph activated phenoloxidase from *Galleria mellonella* (waxmoth larvae) by rhabduscin (**1**), byelyankacin (**2**), and aglycone **3** (aglycone-NC).

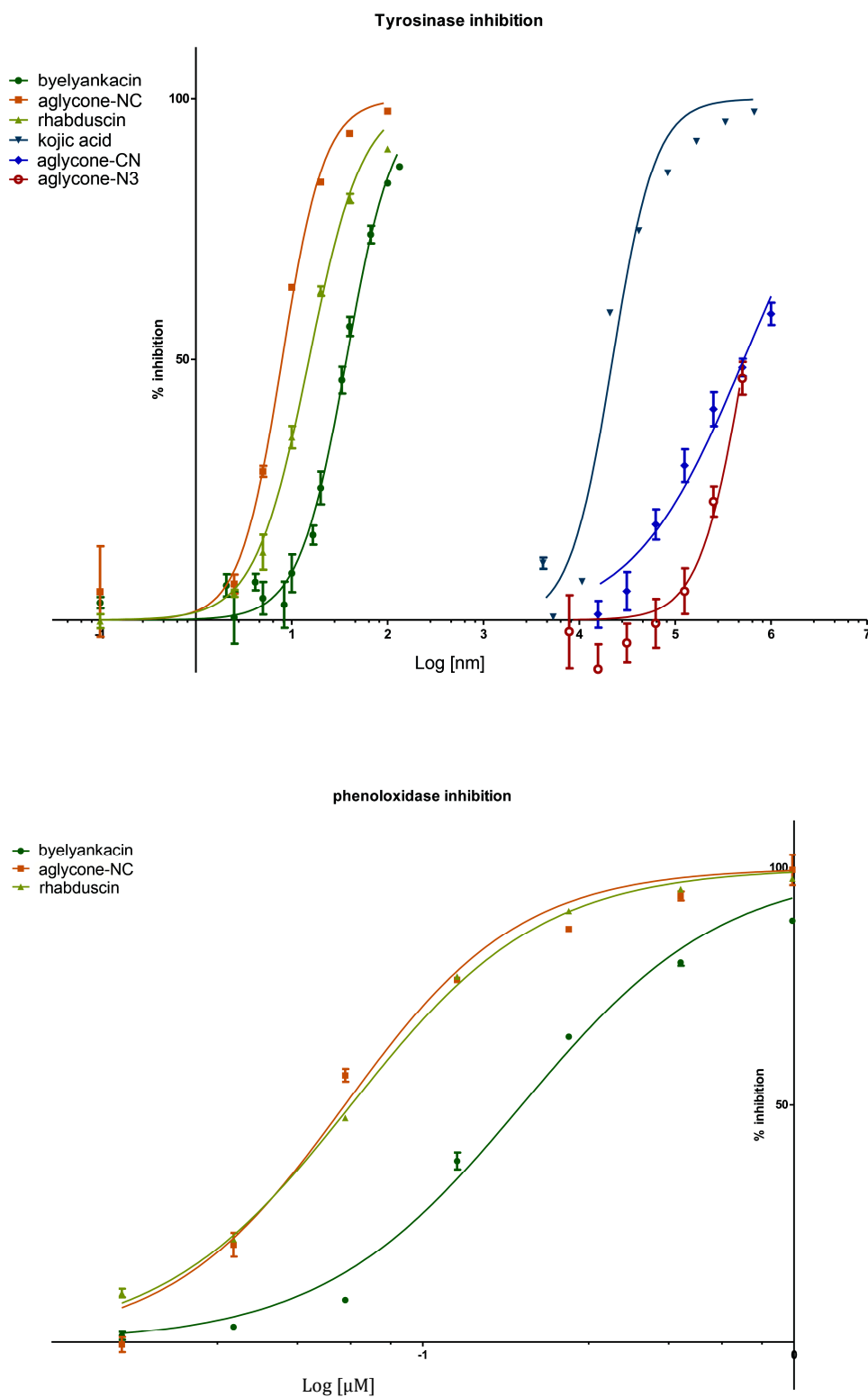


Figure S5. Top: Mushroom tyrosinase inhibition by *X. nematophila* wildtype cells. The OD₆₀₀ of the resuspended washed culture was measured prior to inhibition assay. A small portion of cells was lost during each wash step. **Bottom:** Mushroom tyrosinase inhibition by *X. nematophila* cells normalized to OD₆₀₀. The number of cell washes is plotted on the x-axis.

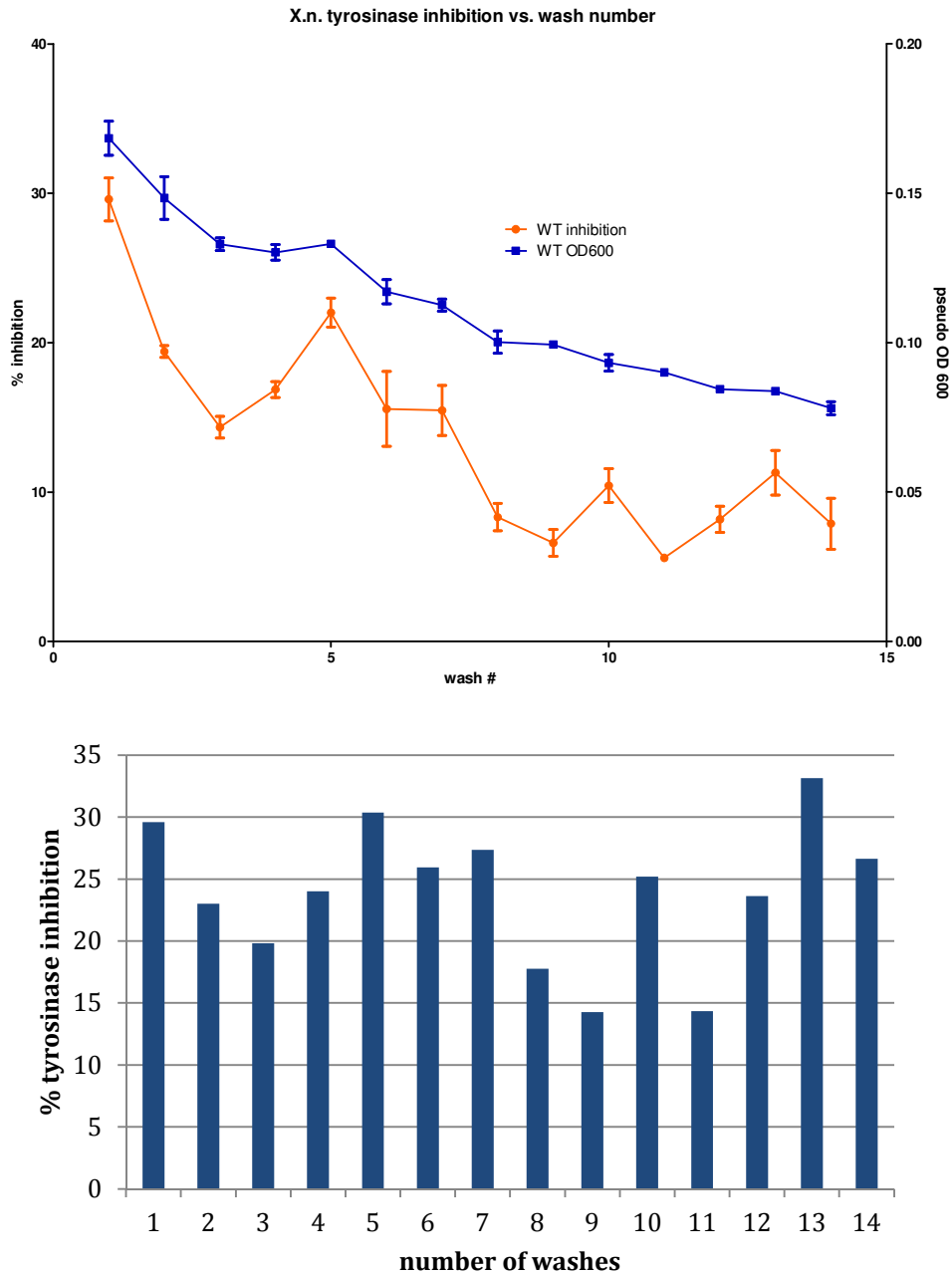
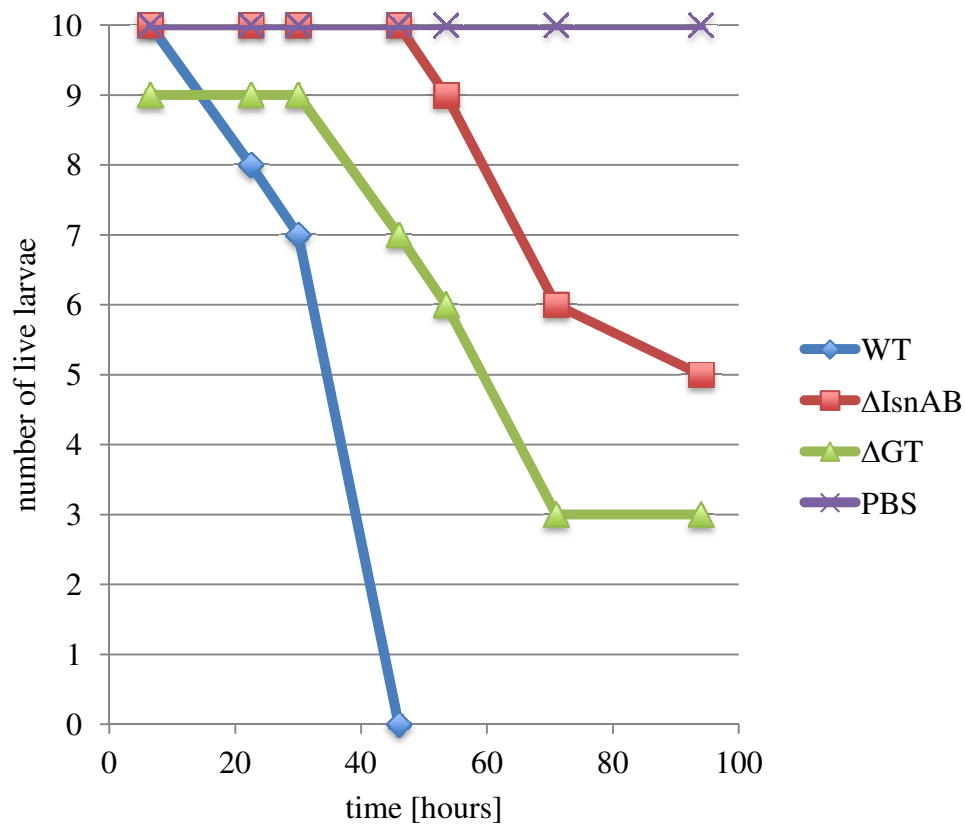


Figure S6. Virulence assays with *Galleria mellonella* larvae (10 larvae per condition) infected with ~10,000 cells of *X. nematophila* wildtype, $\Delta IsnAB$, ΔGT , and a PBS no cell control. At lower cell inoculations (~100 and ~1,000 cells), only wild type was capable of killing the larvae (not shown). One larva in the ΔGT experiment shown below died within an hour after injection likely due to needle puncture wounding. Consequently, this experiment began with 9 larvae rather than 10. Dead larvae are shown below.



X. nematophila $\Delta IsnAB$



X. nematophila ΔGT



X. nematophila wild type

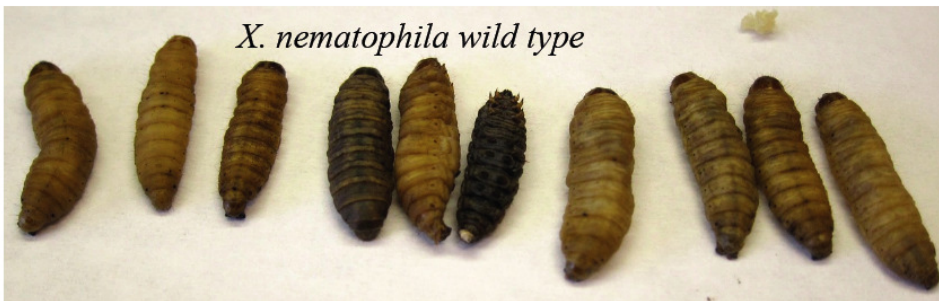
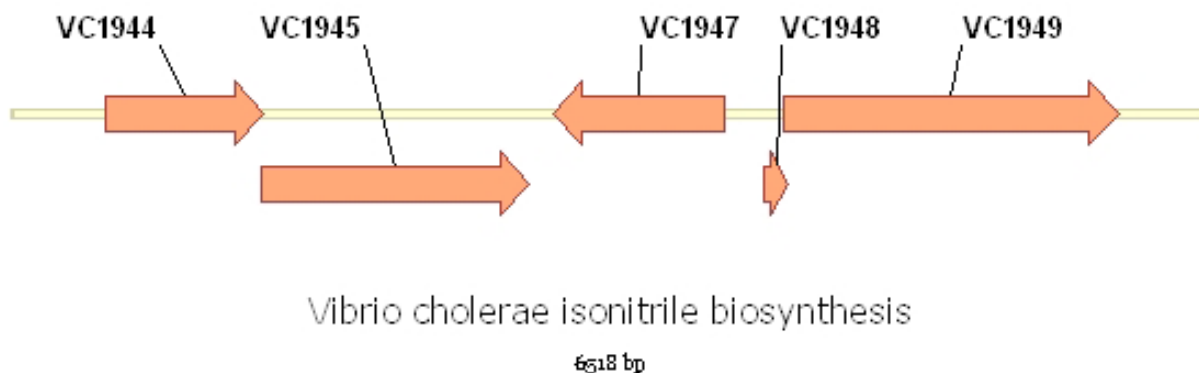


Figure S7A. Zoomed-in view of the isonitrile biosynthetic genes in the *V. cholerae* N16961 genome.



VC1944: IsnB homolog

VC1945: PheA FAD-dependent oxidase homolog

VC1947: LysR-type transcriptional regulator homolog

VC1948: Conserved hypothetical protein

VC1949: IsnA-IsnB fusion homolog

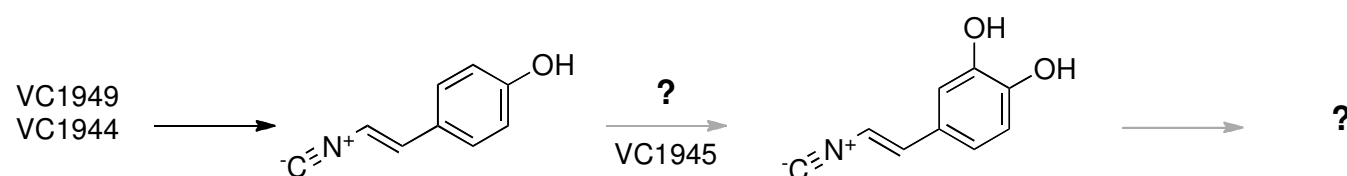


Figure S7B. Selected C₁₈ reversed-phase LC/MS metabolite trace from *E. coli* cultures heterologously expressing *V. cholerae* genes (pJVC1949 and pEVC1944-45). An ethyl acetate extract was fractionated over a C₁₈ SepPak column using methanol gradations for enrichment prior to LC/MS injection. pJVC1949 only when co-transformed with pEVC1944 or pEVC1944-45 led to production of aglycone **3** and its hydrolysis product **3**_{H2O}. The 20% methanol elution (**A**) contains **3**_{H2O} (M-H = 162.1). The 40% methanol elution (**B**) contains both **3** (M-H = 144.0) and **3**_{H2O}. Both **3** and **3**_{H2O} co-elute with standards; top traces in (**A**) and (**B**).

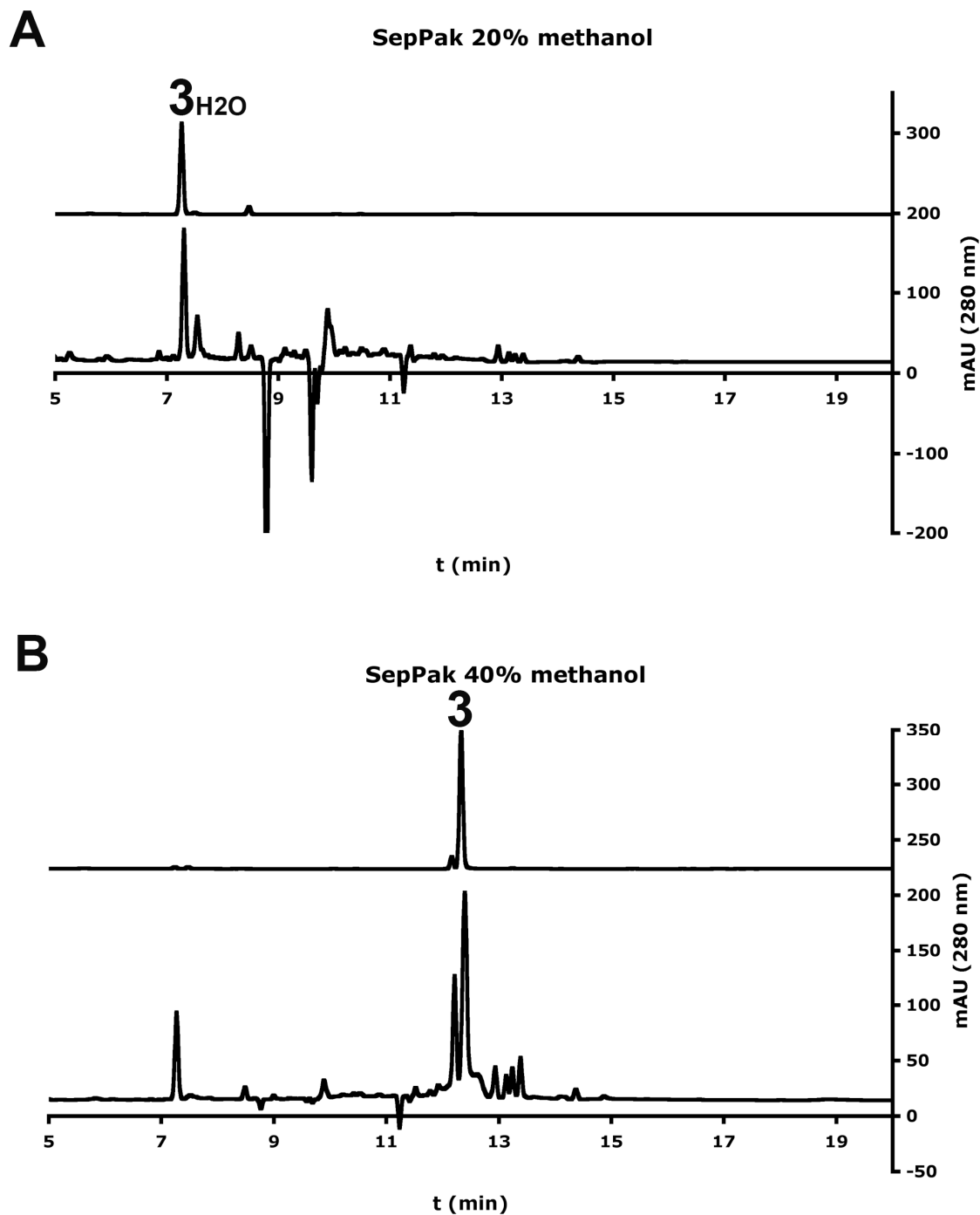


Table S4. Oligonucleotides used in cloning experiments.

Primer	Sequence (5'-3')
<i>X. nematophila</i> oligonucleotides	
IsnAB-A5	gtaaaat-gagctc-tcatgccattcaaaactcccttcata
IsnAB-A3	caatacgcgccattaa-aattcattcctaattgtattgcctccaca
IsnAB-B5	cattaggaatgaatt-ttaatggcgcgtattgttttagctgc
IsnAB-B3	gtaaaat-gagctc-ttgcagtggtccctgagtcacaaa
GT-A5	gtaaaat-gagctc-ttaccctaattatcctgagcaggatattaattc
GT-A3	catccttgtaaaaaaggatc-taattaaacttccttgacagtagaatctattgagtttg
GT-B5	tcaagggaagttaatta-gatcctttttacaaggatgacagaaaaataaac
GT-B3	gtaaaat-gagctc-atacagcgtgaattaatgatttatttttagctc
Isn-5genome	tagttctggtaagggtttttggcg
GT-3genome	cggaaacgattttgacattaccataaggtc
<i>P. luminescens</i> oligonucleotides	
Plu1760-5	gtaaaaat-cat-atggcacgaattgtcattgcagcgg
Plu1760-3	gtaaaaat-ctcgag-ttaattagcacgatttcgaagattaattgtt
Plu1762-5	gtaaaaat-cat-atggcacgtatcatcattgcagcgc
Plu1762-3	gtaaaaat-ctcgag-ttagtgaatgtggcctttgtgcaagaattaat
P.l.-isnA-5XbaI	gtaaat-tctagaaataattttaagaaggagatatac-atgcaaagtgcaccgctaacaattac
P.l.-isnB-3BamHI	gtaaaaatt-ggatcc-ctatgatcttaacgcctgattattaaatgctg
P.l.-isnB-5XbaI	gtaaaat-tctagaaataattttaagaaggagatatac-atgacagaattaaatagcttcagacagaagaa
P.l.-isnA-3BamHI	gtaaaaatt-ggatcc-tcaaattacatagtactgggtttccatg
<i>V. cholerae</i> oligonucleotides	
VC1944-5	gtaaaaat-catatg-gaggccattgatatgccgtacaaa
VC1945-3	gtaaaaat-ctcgag-ctagttagataagtgattctgtcaacacaccttct
VC1944-3	gtaaaaat-ctcgag-ttattttgtggacattggtacgactccaa
VC1945-5	gtaaaaat-catatg-tccacaaaaataaccgacatcgtcat

***X. nematophila* genetics and heterologous expression of *P. luminescens* genes.**

Construction of *X. nematophila* knockout vectors. Deletion constructs for the preparation of scar-less mutants were individually prepared for genes *isnA-isnB* (*Xn_1221-Xn_1222*) and the corresponding glycosyltransferase (*Xn_1223*) in *X. nematophila* ATCC19061. *X. nematophila* gDNA was purified as previously described (Syn, C.K. and Swarup, S. **2000**. *Anal. Biochem.* 278 (1): 86-90). The direct upstream region of *isnA* was amplified by PCR using primer pairs IsnAB-A5 and IsnAB-A3 (Table S4). The direct downstream region of *isnB* was amplified using primer pairs IsnAB-B5 and IsnAB-B3. The upstream and downstream amplification products were used as templates in a final overlap-extension PCR reaction with primer pairs IsnAB-A5 and IsnAB-B3. The product, a fused exchange sequence, cleanly excised the start (*isnA*) through the stop (*isnB*) codons of the *isnA-isnB* region, leaving the downstream glycosyltransferase gene unaffected. The PCR product was digested with SacI and ligated into the corresponding site in pDS132 (Philippe, N., Alcaraz, J.P., Coursange, E., Geiselmann, J.; Schneider, D. **2004**. *Plasmid*. 51 (3):246-255), a suicide plasmid with a chloramphenicol resistance marker, to generate pDΔIsnAB. The deletion construct for glycosyltransferase *Xn_1223* was constructed similarly, using upstream primers (GT-A5 and GT-A3) and downstream primers (GT-B5 and GT-B3). GT-A5 and GT-B3 were used for the subsequent full-length overlap extension PCR reaction. The product was digested with SacI and inserted into pDS132 to generate pDΔGT. To propagate the suicide plasmids, cloning was carried out in the *E. coli* DH5α λ-pir strain (WM3618 λ-pir). Constructs were subjected to restriction analysis and sequencing for verification.

Preparation of deletion mutants. Scar-less deletion mutants of genes *isnA-isnB* and glycosyltransferase *Xn_1223* in *X. nematophila* were prepared using similar conditions as previously described for constructing mutants in the related bacterium, *P. luminescens* (Crawford, J.M., Kontnik, R., Clardy, J. **2010**. *Curr. Biol.* 20 (1):69-74). Deletion constructs pDΔIsnAB and pDΔGT were

transformed into the diaminopimelic acid auxotroph donor *E. coli* strain WM6026 λ -pir by heat-shock. Transformants were selected on LB agar plates supplemented with 25 μ g/mL chloramphenicol. *X. nematophila* ATCC19061 was grown without selection. Donor *E. coli* strains and recipient *X. nematophila* were grown as LB suspension cultures at 37°C and 30°C, respectively, with (or without) appropriate antibiotic supplementation. The suspension cultures were grown to mid-exponential phase ($OD_{600} = 0.5\text{--}0.6$), mixed at a 1:1 and 8:2 donor:recipient ratio (1 mL final), diluted with fresh medium to 5 mL, and filtered (0.2 μ M sterile filter). The filter was transferred to a LB agar plate supplemented with diaminopimelic acid (0.3 mM) and incubated overnight at 30°C. Mating mixtures were individually resuspended in liquid LB and portions were plated on LB agar plates containing 25 μ g/mL chloramphenicol. Single *X. nematophila* colonies growing on the selection plates were re-streaked on LB sucrose (5%) plates lacking chloramphenicol for SacB counter-selection. For both mutants, positives were identified by colony PCR using primer pairs Isn-5genome and GT-3genome (Table S4). Mutants were re-streaked three times on LB sucrose (5%) plates and re-validated to remove any potential wildtype contamination (no larger wildtype PCR bands were observed in the final mutant preparations). The correct-sized PCR products were cloned into pCR2.1 TOPO (Invitrogen) and verified by end-sequencing.

Metabolite analysis of *X. nematophila* wildtype and knockouts. *X. nematophila* wildtype, Δ isnA-isnB, and Δ GT were streaked on LB agar plates and grown for 2 days at 30°C. Two different mutant isolates from each knockout were analyzed, and both showed identical results in the metabolite analysis. Single colonies were individually picked and inoculated into 5 mL of a tryptone/yeast-extract-based medium (2 g tryptone, 5 g yeast extract, and 10 g NaCl per L). The suspension cultures were grown at 30°C and 250 rpm. At 48 h, the organic-extractable metabolites from the whole culture (cells plus spent medium) were rigorously extracted into 5 mL of ethyl acetate, the layers were separated by centrifugation, and the

top 4 mL of ethyl acetate was transferred to a glass vial and dried. The residue was resuspended in 500 μ L methanol and analyzed (40 μ L injections) by LC/MS (Agilent 6130) in both positive and negative ion modes using a Kinetex C₁₈ HPLC column (100 \times 4.60 mm, 100 Å, 2.6 μ m particle size, Phenomenex) with an acetonitrile:water gradient at 0.7 mL/min: 0-2 min, 10% MeCN; 2-25 min, 10-100% MeCN; 25-27 min, 100% MeCN (Figure 2D). The same growth conditions were used for analyzing *X. nematophila* wildtype and *isnAB* mutant with SRS microscopy, except cells were visualized directly at ~48 h growth without manipulation on poly-L-lysine coated microscope slides.

Vector construction for the expression of *P. luminescens* genes in *E. coli*. *P. luminescens* gDNA was purified as previously described (Syn, C.K. and Swarup, S. **2000**. *Anal. Biochem.* 278 (1): 86-90). The *P. luminescens* glycosyltransferase genes *plu1760* and *plu1762* were individually amplified by PCR using primer pairs Plu1760-5/Plu1762-5 and Plu1760-3/Plu1762-3 (Table S4). The amplified products were digested with NdeI and XhoI and inserted into the corresponding sites in pET-Duet (Novagen), just downstream of the second T7 promoter region to generate pEGT1760 and pEGT1762. The *isnA-isnB* (*plu2816-plu2817*) genes were amplified using primer pairs P.l.-isnA-5XbaI and P.l.-isnB-3BamHI and the products were digested with XbaI and BamHI and inserted into the corresponding sites in pET-Duet, pEGT1760, and pEGT1762 just downstream of the first T7 promoter region to generate pEP.l.-IsnAB, pEIsnAB-GT1760, and pEIsnAB-GT1762. The *isnA* (*plu2816*) gene was amplified with P.l.-isnA-5XbaI and P.l.-isnA-3BamHI and inserted into the XbaI/BamHI sites of pET-Duet to yield pEIsnA. The *isnB* (*plu2817*) gene was amplified with P.l.-isnB-5XbaI and P.l.-isnB-3BamHI and similarly inserted into pET-Duet to yield pEIsnB.

Heterologous expression of rhabduscin (1), byelyankacin (2), and the aglycone biosynthetic intermediate 3 (aglycone-NC). BL21(DE3) Star pLysS *E. coli* harboring pEIsnAB-GT1760 was grown overnight in suspension (5 mL of LB, 0.1 mg/mL of ampicillin) from a single colony at 37°C and 250 rpm. Two 1 L batches of M9 minimal medium (0.1 mg/mL of ampicillin) supplemented with 0.5% casamino acids in 4 L Erlenmeyer flasks were inoculated with 5 mL of the overnight stationary phase culture and were grown at 37°C and 250 rpm to an OD₆₀₀ = 0.5-0.6. Expression of the cluster was induced by the addition of IPTG (1 mM final). The cultures were then grown at 25°C and 250 rpm for a final growth time of 24 h. The cells were removed by centrifugation at 4000 × g for 20 min, and each 1 L cleared spent culture was extracted twice with 500 mL of ethyl acetate. The combined organic fraction (2 L) was dried over Na₂SO₄, filtered, and concentrated by rotary evaporation. The compounds were separated by multiple preparative HPLC runs using a Luna C₁₈ column (Phenomenex, 250×21.2 mm, 100 Å, 5 µm particle size) with an acetonitrile:water gradient at 10 mL/min: 0-30 min, 20-60% MeCN; 30-32 min, 60-100% MeCN, 32-40 min, 100% MeCN; prior to the next injection, the column was stabilized for 5 min with 20% MeCN. Retention times: hydrolyzed aglycone **3**_{H₂O}, 12.9 min; rhabduscin (**1**), 18.6 min; byelyankacin (**2**), 19.8 min; and aglycone **3**, 26.9 min. The same growth conditions were used for analyzing *E. coli* strains with SRS microscopy, except cells were grown on a 5 mL scale and visualized directly at ~24 h growth without manipulation on poly-L-lysine coated microscope slides. Product analysis was confirmed by LC/MS for batches analyzed by microscopy.

(E)-4-(2-isocyanovinyl)phenol (3) ¹H NMR and HR-MS. ¹H NMR: (600 MHz, CD₃OD) δ 7.29 (d, *J* = 8.6 Hz, 2H), 6.95 (d, *J* = 14.3 Hz, 1H), 6.77 (d, *J* = 8.7 Hz, 2H), 6.43 (d, *J* = 14.3 Hz, 1H). HR-MS: (ESI) calcd for C₉H₈NO 146.0606 [M+H]⁺, found 146.0612.

(*E*)-N-(4-hydroxystyryl)formamide (3_{H₂O}) NMR and HR-MS. ¹H NMR: (400 MHz, CD₃OD) δ 8.04 (s, 1H), 7.30 (d, *J* = 14.7 Hz, 1H), 7.17 (d, *J* = 8.4 Hz, 3H), 6.72 (d, *J* = 8.6 Hz, 3H), 6.22 (d, *J* = 14.7 Hz, 1H). ¹³C NMR: (100 MHz, CD₃OD) δ 160.73, 157.88, 128.72, 127.91, 119.37, 116.56, 116.33. HR-MS: (ESI) calcd for C₉H₁₀NO₂ 164.0712 [M+H]⁺, found 164.0712.

Rhabduscin (1) ¹H NMR and MS. The ¹H chemical shifts measured were consistent with the previously reported values for rhabduscin (Crawford, et al 2010). ¹H NMR: (600 MHz, CD₃OD) δ 7.41 (d, *J* = 8.7 Hz, 2H), 7.06 (d, *J* = 8.8 Hz, 2H), 7.00 (d, *J* = 14.4 Hz, 1H), 6.53 (d, *J* = 14.4 Hz, 1H), 4.92 (d, *J* = 7.6 Hz, 1H), 4.30 (dd, *J* = 4.7, 1.3 Hz, 1H), 3.95 (qd, *J* = 6.3, 1.4 Hz, 1H), 3.79 (dd, *J* = 10.0, 4.7 Hz, 1H), 3.69 (dd, *J* = 10.0, 7.6 Hz, 1H), 2.05 (s, 3H), 1.17 (d, *J* = 6.4 Hz, 3H). MS: (ESI) (*m/z*) [M+H]⁺ 333.1

Determination of absolute configuration of rhabduscin. The relative configuration for rhabduscin was previously determined by coupling constant analysis (¹H) and ROESY correlations (Crawford, J.M., Kontnik, R., Clardy, J. **2010**. *Curr. Biol.* 20 (1):69-74). To determine the absolute configuration, advanced Mosher ester analysis on rhabduscin was conducted (Hoye, T.R., Jeffrey, C.S., Shao, F. **2007**. *Nat. Protoc.* 2(10):2451-2458). (*R*)-(-)-α-methoxy-α-(trifluoromethyl)phenylacetyl chloride (*R*-MTPA-Cl) and (*S*)-(+)-α-methoxy-α-(trifluoromethyl)phenylacetyl chloride (*S*-MTPA-Cl) was obtained from Sigma-Aldrich. To generate the S-Mosher ester product **M3** (Figure S1), 2.75 mg rhabduscin (**1**, a.k.a. **M1**, 8.3 μmol) was dried by reduced pressure in a 4 mL glass vial containing a Teflon flea magnet. Deuterated pyridine (4 μL) was added and the mixture was partially dissolved in 250 μL of deuterated tetrahydrofuran. Due to poor solubility in most coupling solvents, rhabduscin was only partially dissolved in THF. *R*-MTPA-Cl (1.55 μL, 1 equivalent) was added to the mixture and the reaction

proceeded for 1 h at room temperature. Deuterated acetonitrile was then added (250 μ L) and the reaction continued for an additional 1 h. The reaction mixture was too complex to analyze directly by NMR, so the reaction was completely solubilized in methanol for LC/MS analysis and product purification by semi-preparative HPLC. The *R*-Mosher ester product was synthesized similarly, except 2.62 mg or rhabduscin (7.9 μ mol) was reacted with *S*-MTPA-Cl (1.48 μ L, 1 equivalent). The reaction mixtures were analyzed by LC/MS (Agilent 6130) over a Kinetex C₁₈ HPLC column (100 \times 4.60 mm, 100 Å, 2.6 μ m particle size, Phenomenex) with an acetonitrile:water gradient at 0.7 mL/min: 0-2 min, 10% MeCN isocratic; 2-25 min, 10-100% MeCN; 25-27 min, 100% MeCN (Figure S1). The reaction mixtures included starting materials, rhabduscin-formamide **M2**, rhabduscin Mosher esters (major, **M3**; minor, **M5**), and rhabduscin-formamide Mosher esters (**M4** and **M6**).

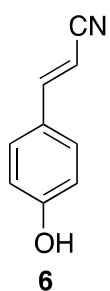
After the synthetic reaction, sample preparation, and processing, the hydrolyzed rhabduscin-formamide Mosher ester (**M4**) was the major product obtained. Consequently, the *R*- and *S*- **M4** products were purified using a semi-preparative Discovery HS C₁₈ HPLC column (25 cm \times 10 mm, 10 μ m particle size, Supelco) with an acetonitrile:water gradient at 2 mL/min: 0-4 min, 20% MeOH isocratic; 4-40 min, 20-68% MeCN; rhabduscin, 10.6 min; major *R*-rhabduscin-formamide Mosher ester **M4** (*S*-MTPA-Cl reaction), 36.9 min; major *S*-rhabduscin-formamide Mosher ester **M4** (*R*-MTPA-Cl reaction), 36.7 min. The Mosher products were analyzed by one-dimensional (¹H) and two-dimensional (gCOSY) NMR (Varian INOVA 600 MHz) using deuterated methanol and an NMR microtube (Shigemi, Inc) susceptibility matched to the solvent (Table S3).

Metabolite analysis of heterologously expressed *P. luminescens* genes. BL21(DE3) Star pLysS *E. coli* transformed with constructs pEIsnA, pEIsnB, pEIsnAB, pEIsnAB-GT1760, pEIsnAB-GT1762, pEGT1760 or pEGT1762 were streaked on LB agar plates containing 0.1 mg/mL ampicillin and grown for 24 h at 37°C. Single colonies were individually picked and inoculated into 5 mL liquid culture (LB,

0.1 mg/mL ampicillin) and grown at 37°C and 250 rpm overnight. Aliquots (5 mL) of liquid medium (M9 minimal medium supplemented with 0.1 mg/mL of ampicillin and 0.5% casamino acids) were then inoculated with 50 μ L of the overnight culture and were grown at 37°C and 250 rpm to an OD₆₀₀ = 0.5-0.6. Expression of the cluster was induced by the addition of IPTG (1 mM final), and the cultures were incubated at 25°C and 250 rpm for a total time of 24 hours. The whole cultures were then extracted with 5 mL ethyl acetate, the organic portions were transferred to glass vials and evaporated under reduced pressure (SpeedVac AES2010), and the residues were resuspended in methanol and subjected to LC/MS analysis (Agilent 6130) in both positive and negative ion modes using a Kinetex C₁₈ HPLC column (100 \times 4.60 mm, 100 Å, 2.6 μ m particle size, Phenomenex) with an acetonitrile 0.1% formic acid (A):water 0.1% formic acid (B) gradient at 0.7 mL/min: 0-2 min, 10% A isocratic; 2-22 min, 10-100% A; 22-27 min, 100% A (Figure 2B). The column was stabilized for 5 min with the initial condition (10% A) prior to the next injection. LC/MS retention times (min) of metabolites produced by *E. coli* transformants harboring *P. luminescens* genes are as follows. Purified standards exhibited identical retention times and masses as expected. Similar growth conditions were used for analyzing *E. coli* by SRS microscopy, except the cells were visualized directly at 24 h growth.

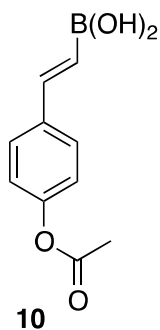
<i>E. coli</i> transformants	3_{H2O}	1	2	3
pEIsnA	-	-	-	-
pEIsnB	-	-	-	-
pEIsnAB	8.3	-	-	13.3
pEIsnAB-GT1760	8.3	10.8	11.2	13.3
pEIsnAB-GT1762	8.3	10.8	11.2	13.3
pEGT1760	-	-	-	-
pEGT1762	-	-	-	-

Synthesis of substrate mimics and precursor directed biosynthesis.



Synthesis of 3-(4-hydroxyphenyl)acrylonitrile (6). The reaction was realized according to a procedure described by N.A. Bumagin and al. (Bumagin, N. A.; More, P. G.; Beletskaya, I. P. *Journal of Organometallic Chemistry* **1989**, 371, 397-401.) In a 10 mL flask under N₂, an orange slurry of water (2 mL), potassium carbonate (0.10 g, 0.75 mmol, 0.75 equivalent), acrylonitrile (0.1 mL, 1.5 mmol, 1.5 equivalent), 4-iodophenol (0.22g, 1.0 mmol, 1.0

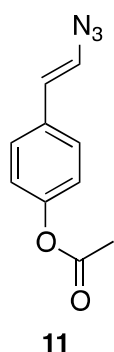
equivalent) and palladium acetate (cat.) was stirred at 90°C. The reaction was followed by TLC (ethyl acetate:hexane 3:7). After 2 hours, more palladium acetate (cat.) was added, and the reaction was stirred for an additional 1.5 h at 90°C. The reaction mixture was then cooled, filtered, acidified with 1N HCl, and extracted with diethyl ether. The combined organic portions were concentrated under reduced pressure, and the resulting residue was purified by chromatography on SiO₂ (ethyl acetate:hexane 3:7) to afford **6** (35 mg, 0.24 mmol, 24%, cis/trans 15/85) as a yellow solid. ¹H-NMR (600MHz, CDCl₃) δ 7.36 (d, *J* = 8.6 Hz, 2 H), δ 7.33 (d, *J* = 16.6 Hz, 1 H), δ 6.86 (d, *J* = 8.6 Hz, 2 H), δ 5.71 (d, *J* = 16.6 Hz, 1 H).



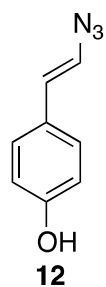
Synthesis of (E)-(4-acetoxystyryl)boronic acid (10). According to a procedure of Q.I. Churches et al. (Churches, Q. I.; Stewart, H. E.; Cohen, S. B.; Shröder, A.; Turner, P.; Hutton, C. A. *Pure Appl. Chem.* **2008**, 80, 687-694.). Under N₂, 1M catecholborane in THF (22.5 mL, 22.5 mmol, 1.2 equivalent) was added to 4-ethynylphenyl acetate (3.0 g, 18.7 mmol, 1 equivalent). The solution was heated at 75°C for 17 h. The reaction

mixture was poured on water (30 mL), and then methanol was added until complete particle dissolution. The solution was heated to reflux for 1.5 h. Methanol was removed under reduced pressure, and the aqueous mixture was extracted with ethyl acetate (3 x 30 mL). The combined organic layers were dried (Na₂SO₄), filtered, and then concentrated under reduced pressure. The residue was purified by chromatography on SiO₂ (CHCl₃:CH₃OH 99:1 → 97:3) to afford a yellow solid (2.49 g). The residue

was purified a second time by chromatography on SiO₂ (CHCl₃:CH₃OH 95:5) to afford **10** (1.61 g, 7.9 mmol, 42%) as a colorless solid. ¹H-NMR: (400 MHz, CD₃OD) δ 7.55 (d, *J* = 8.6 Hz, 2 H), δ 7.32 (d, *J* = 18.1 Hz, 1 H), δ 7.08 (d, *J* = 8.6 Hz, 2 H), δ 6.34 (d, *J* = 18.1 Hz, 1 H), δ 2.27 (s, 3 H). ¹³C-NMR: (100 MHz, CD₃OD) δ 171.0, 152.5, 151.2, 148.3, 137.0, 129.0, 122.9, 20.1. HR-MS: (ESI) calcd for C₁₀H₁₁BO₄Na 229.0648 [M+Na]⁺, found 229.0656.



Synthesis of (E)-4-(2-azidovinyl)phenyl acetate (11). The reaction was adapted from a previously described procedure (Tao, C.-Z.; Cui, X.; Li, J.; Liu, A.-X.; Liu, L.; Guo, Q.-X. *Tetrahedron Lett.* **2007**, 48, 3525-3529). To a mixture of sodium azide (68 mg, 1.05 mmol, 1.2 equivalent) and copper sulfate (14 mg, 0.087 mmol, 0.1 equivalent) in methanol (5 mL) was added **10** (180 mg, 0.87 mmol, 1 equivalent) dissolved in methanol (5 mL). The reaction was stirred at room temperature and followed by TLC (ethyl acetate:hexane 3:7). After 1 h, the reaction mixture was black and all the starting material was consumed. The mixture was directly poured on a silica gel column and the product rapidly eluted (ethyl acetate:hexane 3:7) to afford **11** as a pale orange solid (129 mg, 0.63 mmol, 73%). ¹H-NMR: (400 MHz, CDCl₃) δ 7.27 (d, *J* = 8.5 Hz, 2 H), 7.03 (d, *J* = 8.5 Hz, 2 H), 6.57 (d, *J* = 13.8 Hz, 1 H), 6.25 (d, *J* = 13.8 Hz, 1 H), 2.29 (s, 3H). ¹³C-NMR: (100 MHz, CDCl₃) δ 169.6, 150.0, 133.0, 127.0, 126.9, 122.0, 118.9, 21.2.



Synthesis of (E)-4-(2-azidovinyl)phenol (12). To a solution of (**11**) (9.0 mg, 0.044 mmol, 1 equivalent) in methanol (1 mL) was added potassium carbonate (7.3 mg, 0.053 mmol, 1.2 equivalent) dissolved in water (1 mL). The resulting dark solution was reacted at room

temperature for 15 min. Water (3 mL) was then added and the solution was extracted with ethyl acetate (3 x 5 mL). The combined organic fractions were dried (Na₂SO₄), filtered, and concentrated under reduced pressure to afford (**12**) as a dark brown solid (6.4 mg, 0.038 mmol, 87%). ¹H-NMR: (400 MHz, CD₃OD) δ 7.16 (d, *J* = 8.5 Hz, 2 H), 6.71 (d, *J* = 8.5 Hz, 2 H), 6.66 (d, *J* = 13.8 Hz, 1 H), 6.17 (d, *J* = 13.8 Hz, 1 H). ¹³C-NMR: (100 MHz, CDCl₃) δ 158.1, 128.2, 128.1, 125.3, 120.7, 116.5.

Confocal fluorescence microscopy. 10 μL of cell suspension was deposited on a poly-L-lysine coated microscope slide and covered with a Gold Seal 22×22 mm (No. 1 ½) cover glass. All images were collected with a Nikon A1R confocal mounted on a Nikon Ti-E motorized inverted microscope equipped with a 100x Plan Apo NA 1.4 objective lens and the Perfect Focus System for continuous maintenance of focus. GFP fluorescence was excited with the 488 nm line (selected with a 488/10 filter, Chroma #53044) from a 100 mW Melles Griot argon krypton laser and collected with a triple band pass dichroic mirror (Chroma #53055) and a 525/50 emission filter (Chroma #53051). Images were acquired with a Hamamatsu ORCA ER cooled CCD camera controlled with Nikon Elements software. Brightness, and contrast were adjusted on displayed images (identically for compared image sets) using ImageJ 1.43u software.

Vector construction for the expression of *V. cholerae* genes in *E. coli*. Single colonies of *V. cholerae* El Tor N16961 ΔtxAB::Kan were used as a gDNA template to amplify the desired genes by colony PCR. The standalone *isnB* homolog (*VC1944*) and the downstream oxidase homolog (*VC1945*) were amplified as a single PCR product using primer pairs VC1944-5 and VC1945-3. The product was digested with NdeI and XhoI and inserted into those sites in pETDuet-1 to make pEVC1944-45. *VC1944* was amplified using primers VC1944-5 and VC1944-3 and similarly inserted into pETDuet-1

to create pEVC1944. *VC1945* was amplified with VC-1945-5 and VC-1945-3, and the product was inserted into the NdeI/XhoI sites of pETDuet-1 to generate pEVC1945. A codon-optimized synthon for *E. coli* encoding the amino acid sequence of the apparent *V. cholerae isnA-isnB* fusion gene (*VC1949*) was synthesized by DNA2.0 and inserted into the pJexpress401 vector to make pJVC1949, a kanamycin resistant vector with an inducible T5 promoter. A control vector pJexpress401:27498 (pJ401_RFP_ctrl) expressing red fluorescent protein was also acquired from DNA2.0.

Co-expression experiments.

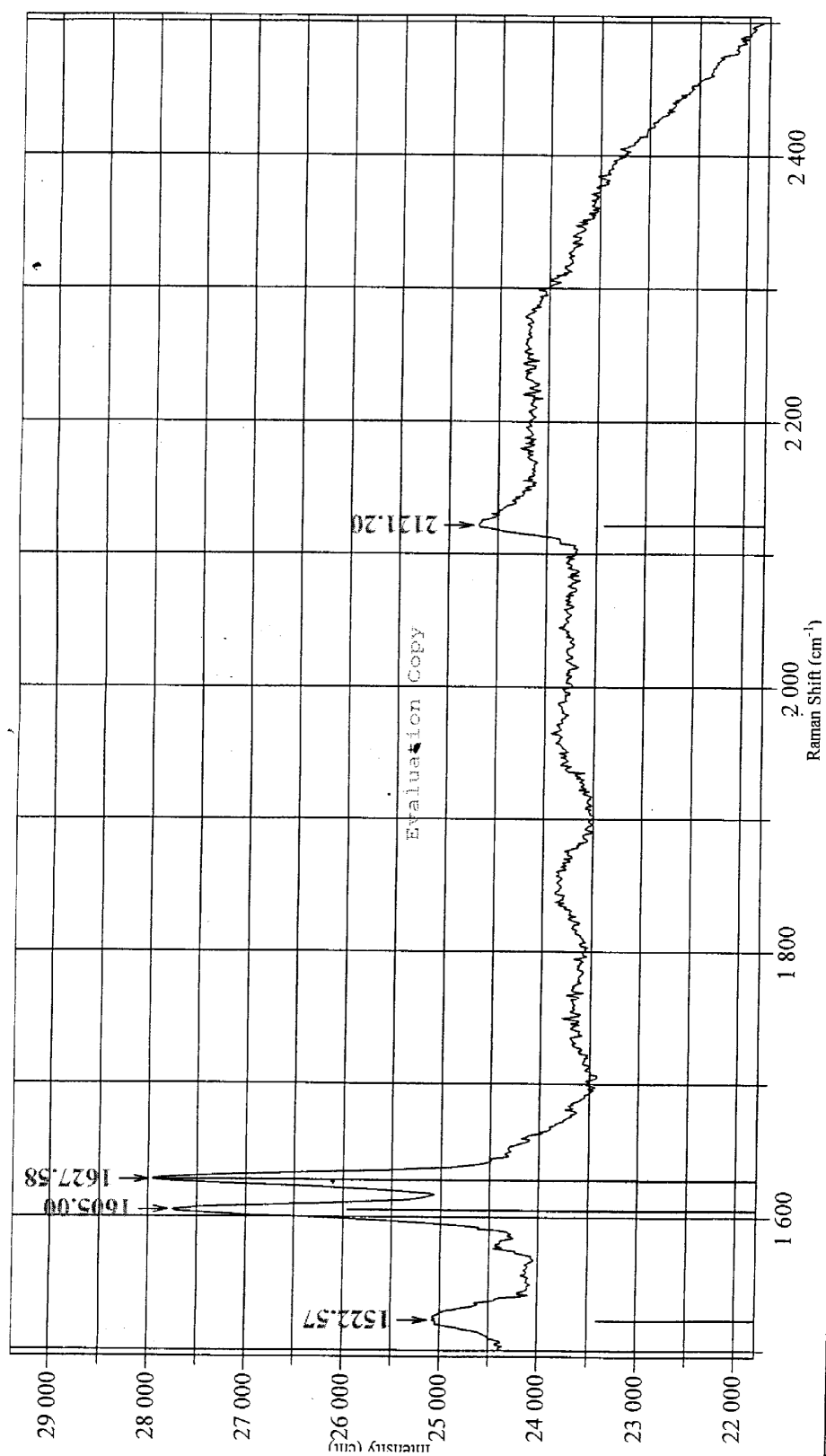
Exp.	Vector 1	Vector 2
Heterologous expression of <i>V. cholerae</i> genes		
1	pJ401_RFP_ctrl (Kanamycin)	
2	pJVC1949 (Kanamycin)	
3	pEVC1944 (Ampicillin)	
4	pEVC1945 (Ampicillin)	
5	pEVC1944-45 (Ampicillin)	
6	pAVC1945 (Chloramphenicol)	
7	pJVC1949 (Kanamycin)	pEVC1944 (Ampicillin)
8	pJVC1949 (Kanamycin)	pEVC1945 (Ampicillin)
9	pJVC1949 (Kanamycin)	pEVC1944-45 (Ampicillin)
10	pJ401_RFP_ctrl (Kanamycin)	pEVC1944-45 (Ampicillin)
Heterologous expression of <i>V. cholerae</i> and <i>P. luminescens</i> genes		
11	pEP.l.-IsnAB (Ampicillin)	
12	pEIsnAB-GT1760 (Ampicillin)	
13	pEIsnAB-GT1762 (Ampicillin)	
14	pEP.l.-IsnAB (Ampicillin)	pAVC1945 (Chloramphenicol)
15	pEIsnAB-GT1760 (Ampicillin)	pAVC1945 (Chloramphenicol)
16	pEIsnAB-GT1762 (Ampicillin)	pAVC1945 (Chloramphenicol)

Codon-optimized VC1949.

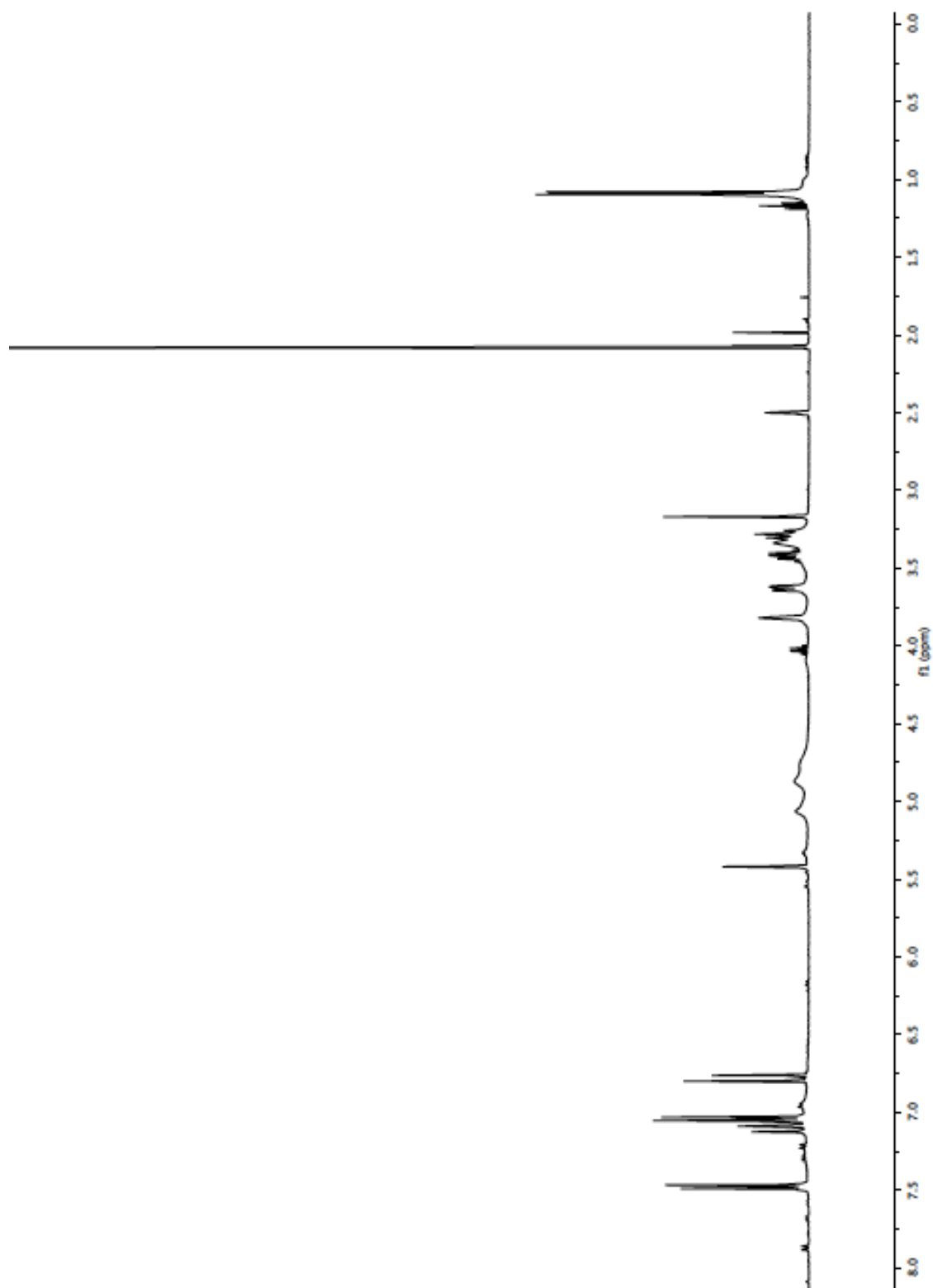
ATGCTGGATGCACAACAAGAAACGTACGTCGAGAAAATCAGCTTCATTCTGCTGAACCAGC
 TGATTGCGCAGTGTAATGCT
 AGCTACAATGGTTTGGCGCACCTGAAGAGCCAAATCCGTCGCTTTGTAACTCCCAAGAGA
 AGATCAAACCTGCTGTTGCCG
 GCCTTTCCGTGTAAAACGAATAATCTGGATAAAGTCCTGAGCCATACCCCGGATCTGGGCG
 AGTATGTGGTGCTGCGCAAG
 TTTGTGCAGTGTATTCGTGATATCGAGAGCGTCTACGAGCCGGGTGTCACCTTTTACATTTT
 CTCTGATTATCACACCTTT
 TCCGACTACATTAGCGTGGACCTGGATCACCACCTATGACTATAGCGATAACCTGCGTAAGA
 TGGTTGCGAATATGAACTGC
 AGCGATGCGTTGAAAATCGTGAACCTTCGAGCATTTTGACGAGTTTAGCGACTTGAAAGATA
 CGGAGTATTTTCGACGGCCTG
 CGTGAAAAGTTTCGGCGACCCTGACTATGCCGAGAATTTACCCGAGCTGAACTGAAGAACA
 ATAAGATGAATCAAACCTAT
 CTGGGCTTGAAAAAGTTTCATGAATCAAGACCAAAAAGTTCGTTTTGGCGCCGTTGTCCTACA
 AAGACCGCCGTCGCCGCCTG
 GCCGACATCGCTAAGGGTATGATGGTCCAGGGTAAAGCGTTGGACAACCTTTTTGCAACAGA
 AATTCGCGGACTGCATTCGT
 CTGAGCATCCATGAACACCCGATGATTGGTAAGAAATACTCTCTGTTTCTGTTTCATGAACG
 CCAATTCAAACCCCGTGG
 CATAGCACGCTGCTGTTTCGACGCAAGCCGCGGTGAGTTCATTATTGACAGCAAGGAAAATC
 ATCTGAAACGTTTCGGGTGTG
 ATTCTGCCGGTACCCACGACGGTAAGCCGTGGTGCTACCTGCAGCTGTCCGCAGCTGACG
 AGGTGCATGCGCACGCACTG

CGCCAAATTCGTGCGGAGCTGCAGCACGAGAAAAGCGGCCTGTACCTGGAATGTCCGGCG
AACCGTGCAAGCCTGGACATG
CTGCTGCCAAAGGAGCTGTCCCAACTGGTGAAGGAGTTTGGTTCTGTTCTGCTGCGTGGTTT
TGCGCCGTTGGCGGACGCC
GAACAGCTGCAAACCTTGGTATCTGAATCATCGTAGCGCGGTGACTTGGGCATACGAAGTGA
GCGTTCAGGCGTTTAAAGGT
AGCGCGGGTGAACAACCGTTGCATTGGGAACTGAGCTGCCCTCCGGCATATATGGCAGTCC
ACCCGCACCGCTATCAGTAC
GAGGATTACACCCCGCACGAGTATGCGGTTTACTCTGTGCGCAAGCCCTGATAGCAATACCT
GGACGGTTGTTGATGCCGCC
TTGGCCGTCCTGACCATCAATGGCCAGGAACGTGAGCAGCTGCGTAACACCATCATGCATT
ACAGCAACTTCAGCCCAGAG
CATGGCGGCAACACCTTGCACCCGCTGGTTCGTTATTGTAGCACCAGCCGTCAGGATGTTCT
GCGTTGGCAGGATTTCCAG
CACGCACAGGGTTATCTGACCCACCTGGAAGGCGTTAGCGAACTGACGGAACAAAGCCGC
GTGTACCAGCGTCTGAACACG
CTGTGCCACGACCCGCGTGTATGCTTCGAGTACCGCCTGCAAACGGGTGATCTGCTGCTGG
TGAATAACCTGACCACCCTG
CAGGCTAGCCACACGTCTAGCATGCACAACGAATACTGGTCCATTACCTGCAGCCGGATT
CGATCAACAGCCCGTGGCAG
CCGCATAACCGTATCGTTGAACAAGCTGAACTGACGTCCGCGTAA

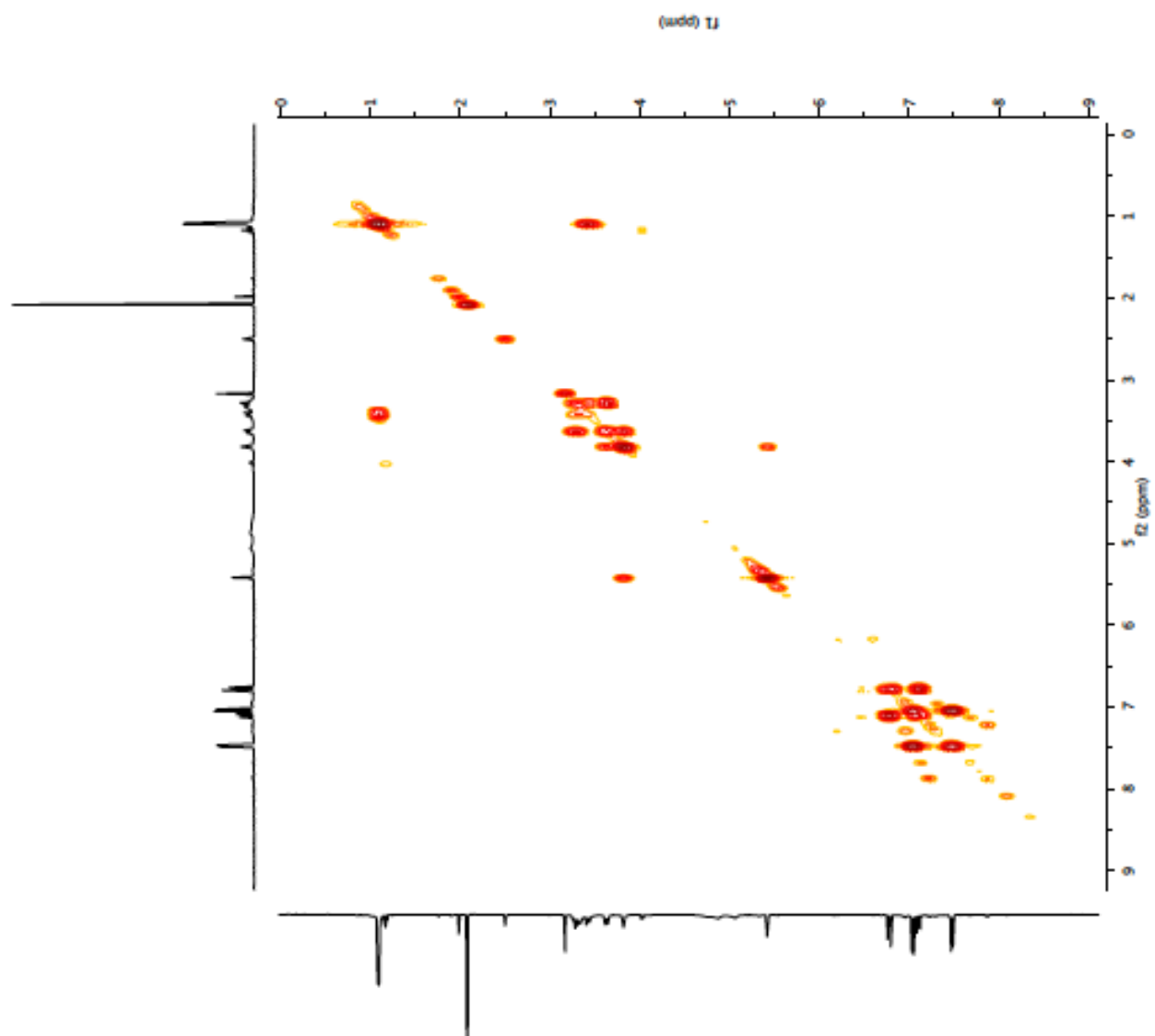
Rhabduscin Raman Spectrum



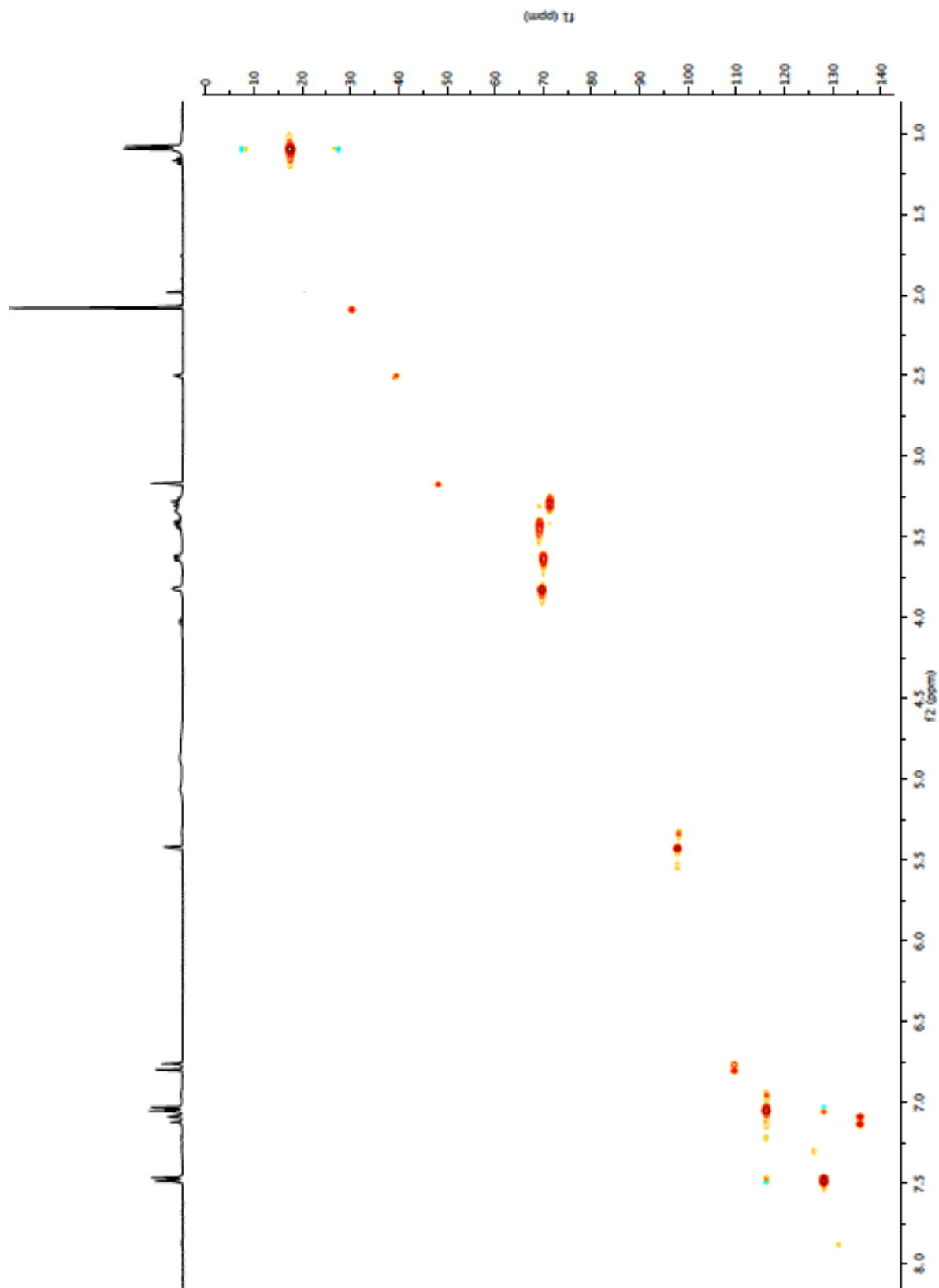
^1H NMR spectrum of byelyankacin (2) in $\text{DMSO-}d_6$ (600MHz)



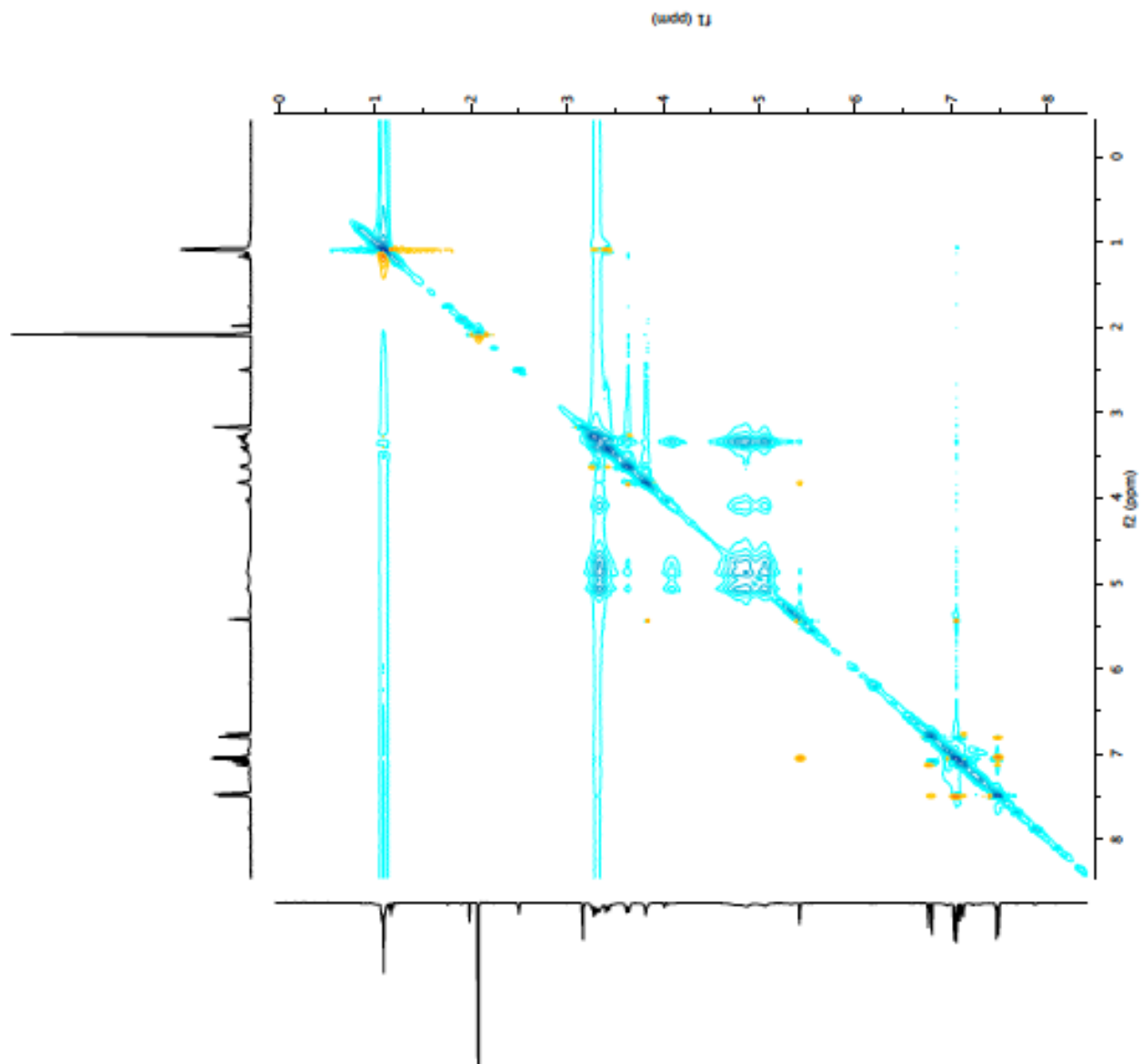
gCOSY NMR spectrum of byelyankacin (2) in DMSO-*d*₆ (600MHz)



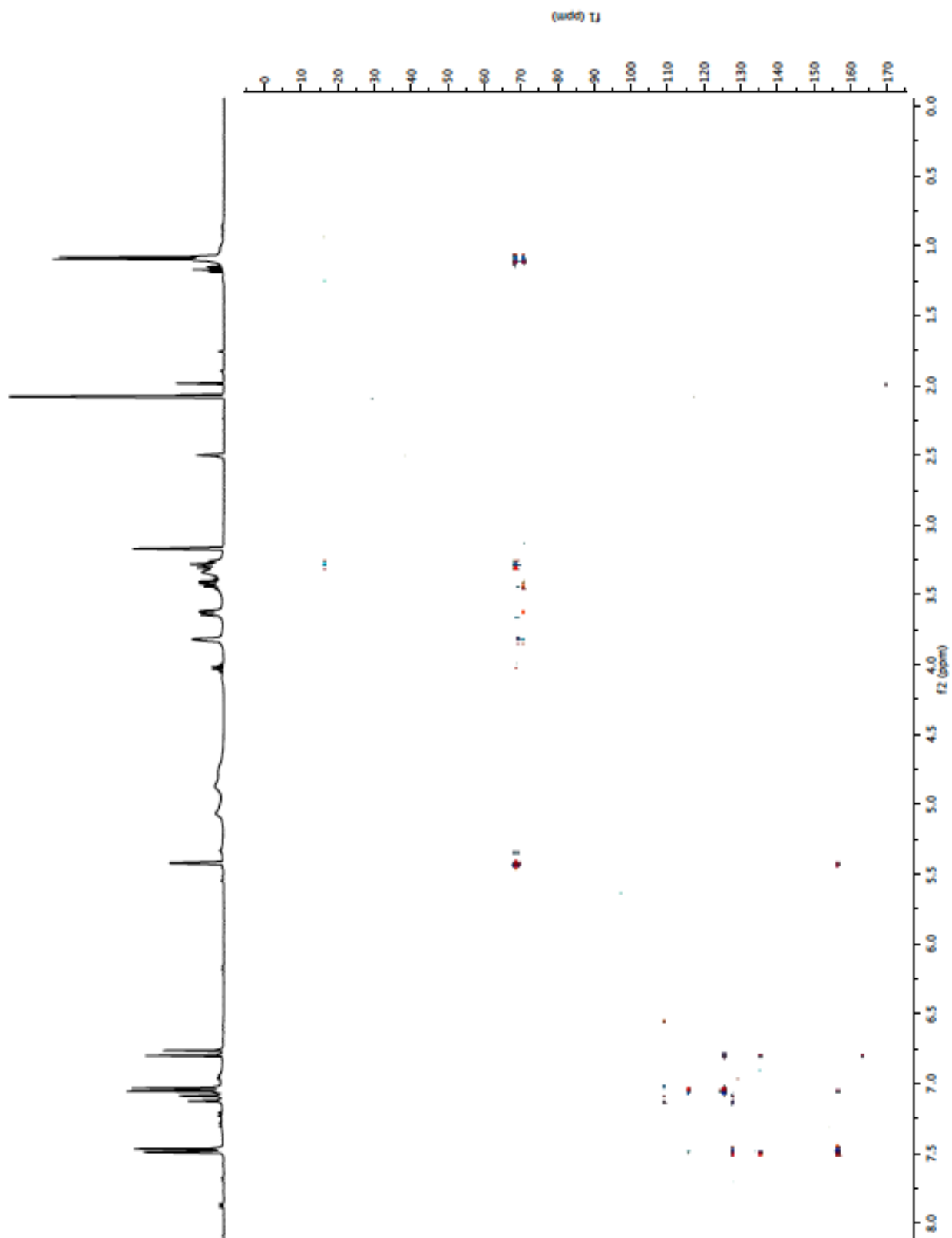
HSQC NMR spectrum of byelyankacin (2) in DMSO- d_6 (600MHz)



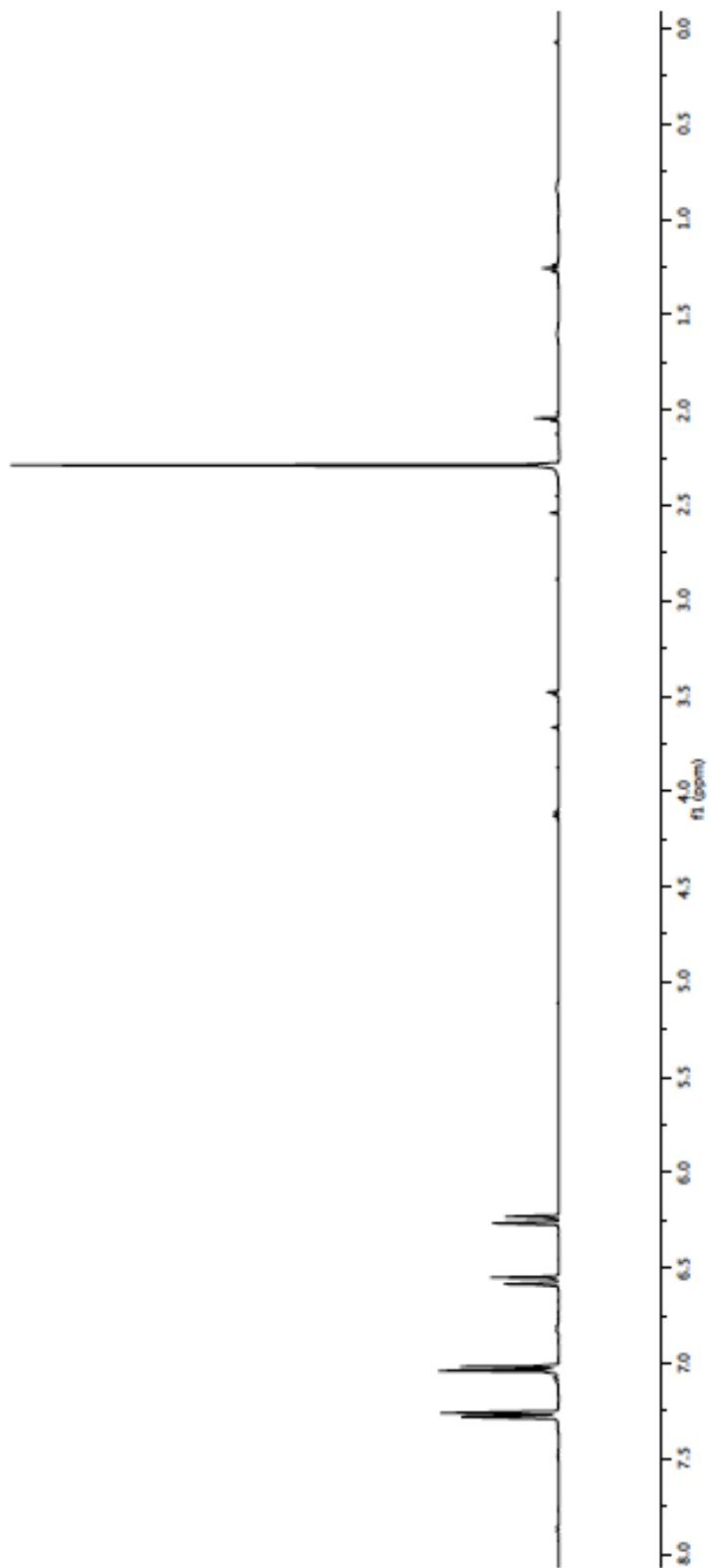
NOESY NMR spectrum of byelyankacin (2) in DMSO- d_6 (600MHz)



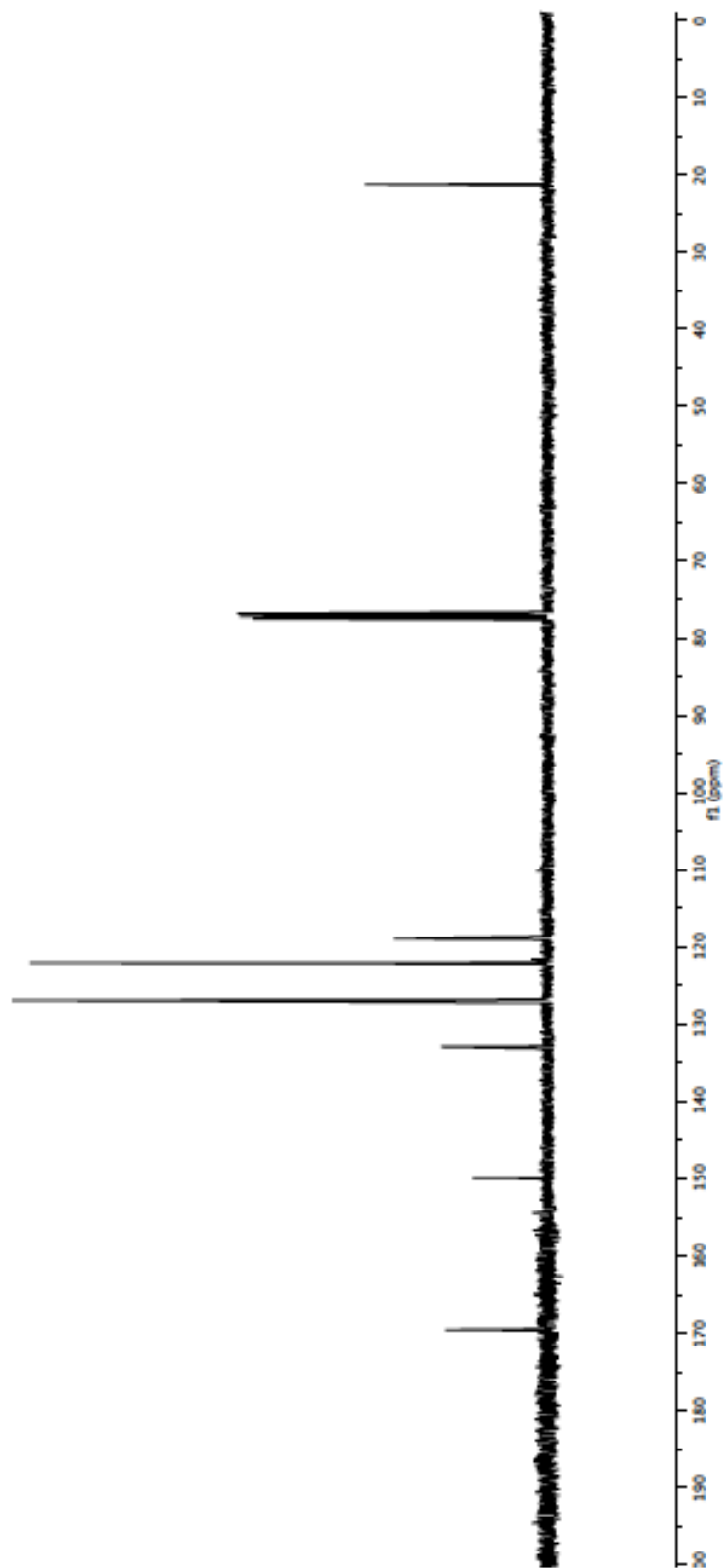
gHMBC NMR spectrum of byelyankacin (2) in DMSO-*d*₆ (600MHz)



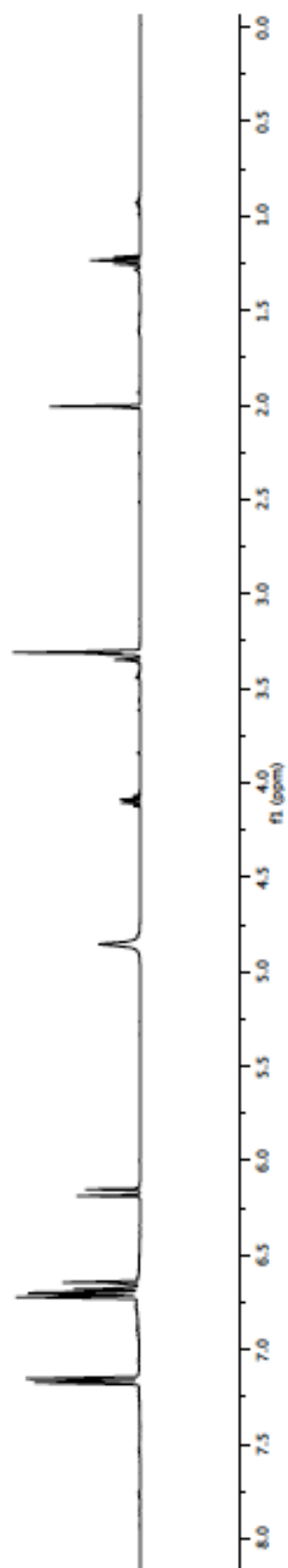
^1H NMR spectrum of (*E*)-4-(2-azidovinyl)phenyl acetate (11) in CDCl_3 (400MHz)



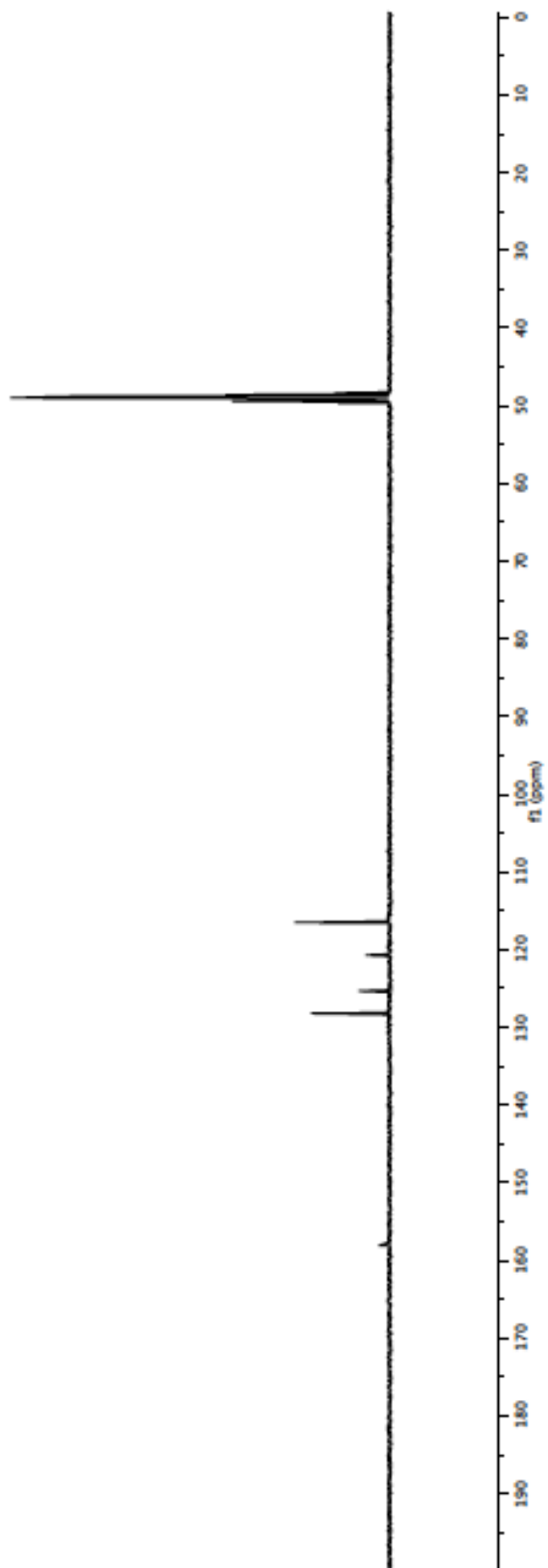
^{13}C NMR spectrum of (*E*)-4-(2-azidovinyl)phenyl acetate (11) in CDCl_3 (100MHz)



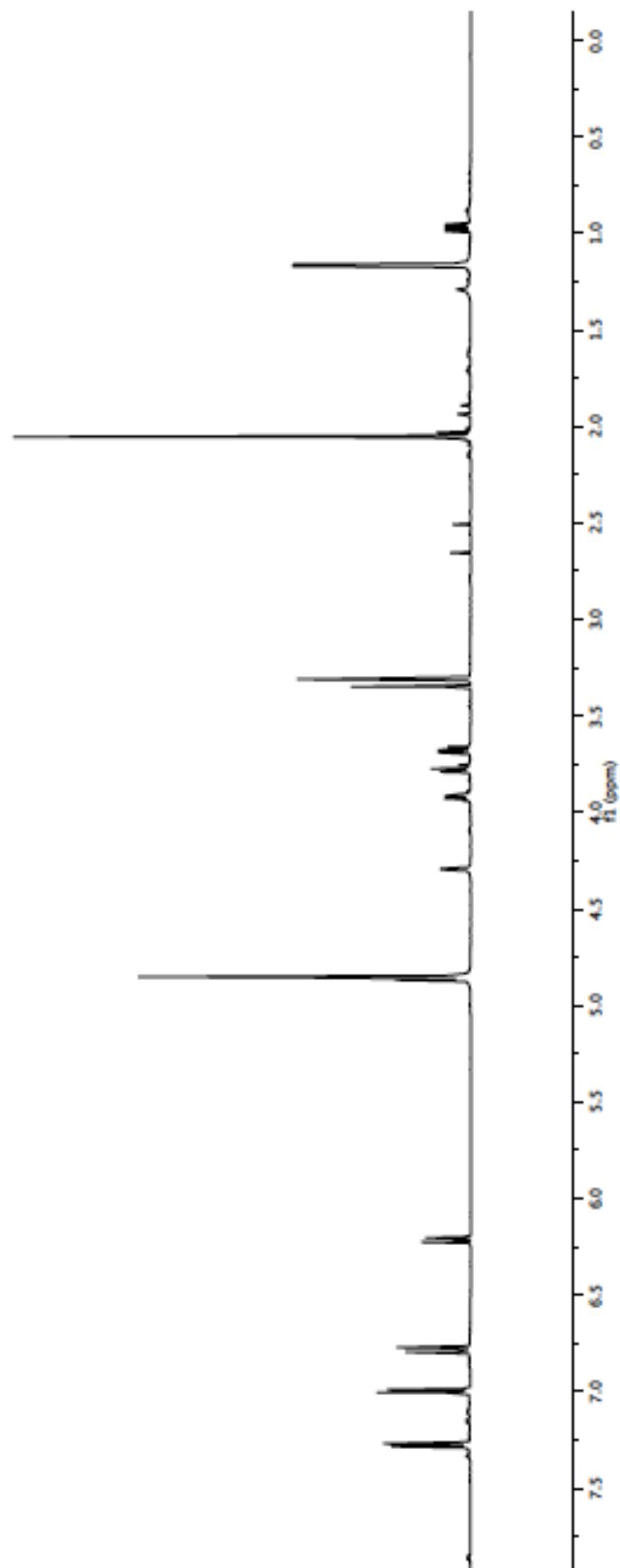
^1H NMR spectrum of (*E*)-4-(2-azidovinyl)phenol (12) in CD_3OD (400MHz)



^{13}C NMR spectrum of (*E*)-4-(2-azidovinyl)phenol (12) in CD_3OD (100MHz)



^1H NMR spectrum of rhabduscin-azide (13) in CD_3OD (600MHz)



^{13}C NMR spectrum of rhabduscin-azide (13) in CD_3OD (150MHz)

